Theoretical and Applied Mechanics Letters 13 (2023) 100430

Contents lists available at ScienceDirect

Theoretical and Applied Mechanics Letters

journal homepage: www.elsevier.com/locate/taml

Letter

Path integral solutions for n-dimensional stochastic differential equations under α-stable Lévy excitation

Wanrong Zan[a], Yong Xu[b,c,*], Jürgen Kurths[d,e]

[a] School of Mathematics, Northwest University, Xi'an, 710127, China
[b] Department of Applied Mathematics, Northwestern Polytechnical University, Xi'an, 710129, China
[c] MIIT key Laboratory of Dynamics and Control of Complex Systems, Northwestern Polytechnical University, Xi'an, 710129, China
[d] Potsdam Institute for Climate Impact Research, Potsdam, 14412, Germany
[e] Department of Physics, Humboldt University of Berlin, Berlin, 12489, Germany

ARTICLE INFO

Article history:
Received 16 November 2022
Revised 20 December 2022
Accepted 4 January 2023
Available online 21 January 2023

Keywords:
Path integral method
α-stable Lévy noise
Monte carlo method
Fokker-Planck-Kolmogorov equation

ABSTRACT

In this paper, the path integral solutions for a general n-dimensional stochastic differential equations (SDEs) with α-stable Lévy noise are derived and verified. Firstly, the governing equations for the solutions of n-dimensional SDEs under the excitation of α-stable Lévy noise are obtained through the characteristic function of stochastic processes. Then, the short-time transition probability density function of the path integral solution is derived based on the Chapman-Kolmogorov-Smoluchowski (CKS) equation and the characteristic function, and its correctness is demonstrated by proving that it satisfies the governing equation of the solution of the SDE, which is also called the Fokker-Planck-Kolmogorov equation. Besides, illustrative examples are numerically considered for highlighting the feasibility of the proposed path integral method, and the pertinent Monte Carlo solution is also calculated to show its correctness and effectiveness.

In almost all fields, such as physics, chemistry, biology, meteorology, finance, and engineering, uncertainty is inevitable, and the system can be modeled and characterized by stochastic differential equation (SDE) [1,2]. One of the most important example is the Langevin equation, which describes how a system evolves when subjected to both deterministic and random forces. The earliest and classical application is Brownian motion, which models the motion of Brownian particles in fluid under random impacts of surrounding fluid molecules. Afterwards, the systems driven by Gaussian white noise (or Brownian motion) make extensive and in-depth progress in both theory and dynamical behaviours [3]. In addition, systems under Poisson and Lévy noise excitations have also received attention due to the diversity of random factors [4–6]. For the response uncertainty of these systems, probability and statistics are powerful tools for system analysis.

Starting from the SDE, we can simulate the sample path of the equation, and then obtain the mean, variance or approximate the probability density function of the response by statistical methods. Besides, it is also possible to first derive the equation satisfied by the probability density function of the response of the SDE, which is called the Fokker-Planck-Kolmogorov (FPK) equation. The FPK equation for systems under Gaussian noise, Poisson and α-stable Lévy noise are second-order, integral-differential and fractional partial differential equations, respectively [7–9]. As partial differential equation, the FPK equation can be solved by finite difference method, finite element method and spectral method, etc. It can obviously be solved by the path integral method specific to random problems, which is a functional integration that includes all random sample paths. The path integral solution is both the solution of the FPK equation and the probability density function of the solution of the SDE. Compared with the statistical methods, the path integral method is not affected by the number of sample paths, and has higher precision, especially in the tail part of the probability density function, which is very useful for the study of the response of random systems and rare events.

The earliest use of the path integral method for response of SDE goes back to 1983, when Wehner and Wolf presented an efficient numerical path integral method to solve nonlinear governing equation of SDE with Gaussian noise [10]. Extension of the path integral

* Corresponding author.:.
E-mail address: hsux3@nwpu.edu.cn (Y. Xu).

https://doi.org/10.1016/j.taml.2023.100430

method to restrictive stochastic processes and time dependent coefficients case shows their wide applicability [11]. After that, the path integral method under Gaussian noise excitation has made a series of research progress in system response, algorithm improvement, etc. [12–16]. In recent years, it has also even been extended to the case of non-Gaussian noise excitation [17–21]. The path integral method for SDE under α-stable Lévy noise is now available for one-dimensional and single-degree-of-freedom(SDOF system. But an open question is whether it can be directly generalized to n-dimensional systems like the Monte Carlo method, which seems to be currently the only method for solving higher-dimensional SDEs under Lévy noise excitation and obviously applicable to systems of arbitrary dimensions? In this paper, we provide a more general path integral formulation for a general n-dimensional SDE under α-stable Lévy excitation.

Considering the following n-dimensional Itô SDE

$$\begin{cases}\dot{\boldsymbol{X}}(t)=\boldsymbol{f}(\boldsymbol{X},t)+\boldsymbol{g}(\boldsymbol{X},t)\boldsymbol{\xi}(t),\\ \boldsymbol{X}(t_0)=\boldsymbol{x}_0,\end{cases} \tag{1}$$

here $\boldsymbol{X}(t)=[X_1(t),X_2(t),\cdots,X_n(t)]^{\mathrm{T}}$ is an n-dimensional state vector, $\boldsymbol{f}(\boldsymbol{X},t)$ is an n-dimensional vector function $[f_1(\boldsymbol{X},t), f_2(\boldsymbol{X},t),\cdots,f_n(\boldsymbol{X},t)]^{\mathrm{T}}$, and $\boldsymbol{g}(\boldsymbol{X},t)=\mathrm{diag}(g_1(\boldsymbol{X},t),g_2(\boldsymbol{X},t),\cdots, g_n(\boldsymbol{X},t))$. $\boldsymbol{X}(t_0)=\boldsymbol{x}_0=[x_{0,1},x_{0,2},\cdots,x_{0,n}]^{\mathrm{T}}$ is the initial condition, which can be deterministic or stochastic. $\boldsymbol{\xi}(t)=[\xi_{\alpha_1}(t),\xi_{\alpha_2}(t),\cdots,\xi_{\alpha_n}(t)]^{\mathrm{T}}$ and $\xi_{\alpha_j}(t)(j=1,2\cdots,n)$ are mutually independent symmetric α-stable Lévy noise, which is the formal derivative of symmetric α-stable Lévy process $L_{\alpha_j}(t)$. $L_{\alpha_j}(t)\sim S_{\alpha_j}(\sigma_j t^{1/\alpha},0,0)$ with characteristic function $Z(k)=\exp[\mathrm{i}kL_{\alpha_j}(t)]=\exp(-D_{L_j}t|k|^{\alpha_j})$, where $D_{L_j}=\sigma_j^{\alpha_j}$ is the noise intensity. And, the characteristic function for the increment of $L_{\alpha_j}(t)$ is $\delta Z_{L_{\alpha_j}}(k,\delta t)=\exp\left(-\delta tD_{L_j}|k|^{\alpha_j}\right)$ (δt is the time increment), which corresponding to the distribution $S_{\alpha_j}(\sigma_j\delta t^{1/\alpha},0,0)$.

For the Markov Process, the Chapman-Kolmogorov-Smoluchowski (CKS) equation holds. Namely, for any $\delta t>0$

$$p(\boldsymbol{x},t+\delta t|\boldsymbol{x_0},t_0)=\int_{R^n}p(\boldsymbol{x},t+\delta t|\boldsymbol{y},t)p(\boldsymbol{y},t|\boldsymbol{x_0},t_0)\mathrm{d}\boldsymbol{y}, \tag{2}$$

where $p(\boldsymbol{x},t+\delta t|\boldsymbol{x_0},t_0)$ and $p(\boldsymbol{y},t|\boldsymbol{x_0},t_0)$ are probability density functions at time $t+\delta t$ and t, with the initial condition $\boldsymbol{X}(t_0)=\boldsymbol{x}_0$. $p(\boldsymbol{x},t+\delta t|\boldsymbol{y},t)$ is the transition probability density function from the position $\boldsymbol{y}$ at the time t to the position $\boldsymbol{x}$ at the time $t+\delta t$.

In the above CKS equation, the transition probability density function $p(\boldsymbol{x},t+\delta t|\boldsymbol{y},t)$ can be represented as

$$\begin{aligned}p(\boldsymbol{x},t+\delta t|\boldsymbol{y},t)&=\mathcal{F}^{-1}[\delta Z_{\boldsymbol{X}}(\boldsymbol{k},\delta t|\boldsymbol{y},t)]\\&=\mathcal{F}^{-1}[\exp(\delta K_{\boldsymbol{X}}(\boldsymbol{k},\delta t|\boldsymbol{y},t))]\\&=\int_{R^n}\frac{1}{(2\pi)^n}\exp\left[-\mathrm{i}\boldsymbol{k}^{\mathrm{T}}(\boldsymbol{x}-\boldsymbol{y})\right]\exp[\delta K_{\boldsymbol{X}}(\boldsymbol{k},\delta t|\boldsymbol{y},t)]\mathrm{d}\boldsymbol{k}.\end{aligned} \tag{3}$$

Among which, $\mathcal{F}^{-1}$ is the Fourier inverse transformation and $\boldsymbol{k}$ is the conjugate variable of $\boldsymbol{x}-\boldsymbol{y}$. In the above, $\delta Z_{\boldsymbol{X}}(\boldsymbol{k},\delta t|\boldsymbol{y},t)$ and $\delta K_{\boldsymbol{X}}(\boldsymbol{k},\delta t|\boldsymbol{y},t)$ are the characteristic function and cumulant generating function of the transition probability density function $p(\boldsymbol{x},t+\delta t|\boldsymbol{y},t)$.

Substituting Eq. (3) into Eq. (2), we get

$$\begin{aligned}p(\boldsymbol{x},t+\delta t|\boldsymbol{x_0},t_0)=&\int_{R^n}\int_{R^n}\frac{1}{(2\pi)^n}\exp\left[-\mathrm{i}\boldsymbol{k}^{\mathrm{T}}(\boldsymbol{x}-\boldsymbol{y})\right]\\&\exp[\delta K_{\boldsymbol{X}}(\boldsymbol{k},\delta t|\boldsymbol{y},t)]p(\boldsymbol{y},t|\boldsymbol{x_0},t_0)\mathrm{d}\boldsymbol{k}\mathrm{d}\boldsymbol{y}.\end{aligned} \tag{4}$$

Letting $\delta t=0$, Eq. (4) reduces to

$$p(\boldsymbol{x},t|\boldsymbol{x_0},t_0)=\int_{R^n}\int_{R^n}\frac{1}{(2\pi)^n}\exp\left[-\mathrm{i}\boldsymbol{k}^{\mathrm{T}}(\boldsymbol{x}-\boldsymbol{y})\right]p(\boldsymbol{y},t|\boldsymbol{x_0},t_0)\mathrm{d}\boldsymbol{k}\mathrm{d}\boldsymbol{y}. \tag{5}$$

Using Eq. (4) minus Eq. (5), we get

$$\begin{aligned}&p(\boldsymbol{x},t+\delta t|\boldsymbol{x_0},t_0)-p(\boldsymbol{x},t|\boldsymbol{x_0},t_0)\\&=\int_{R^n}\int_{R^n}\frac{1}{(2\pi)^n}\exp\left[-\mathrm{i}\boldsymbol{k}^{\mathrm{T}}(\boldsymbol{x}-\boldsymbol{y})\right]\{\exp[\delta K_{\boldsymbol{X}}(\boldsymbol{k},\delta t|\boldsymbol{y},t)]-1\}\\&\quad p(\boldsymbol{y},t|\boldsymbol{x_0},t_0)\mathrm{d}\boldsymbol{k}\mathrm{d}\boldsymbol{y}.\end{aligned} \tag{6}$$

Besides, the characteristic function for the increment of the solution $\boldsymbol{X}(t)$ of the SDE (1) is

$$\begin{aligned}\delta Z_{\boldsymbol{X}}(\boldsymbol{k},\delta t|\boldsymbol{y},t)&=\exp[\delta K_{\boldsymbol{X}}(\boldsymbol{k},\delta t|\boldsymbol{y},t)]\\&=E\left\{\exp\left[\mathrm{i}\boldsymbol{k}^{\mathrm{T}}(\boldsymbol{X}(t+\delta t)-\boldsymbol{X}(t))\right]|\boldsymbol{X}(t)=\boldsymbol{y}\right\}\\&=E\left\{\exp\left[\mathrm{i}\boldsymbol{k}^{\mathrm{T}}(\boldsymbol{f}(\boldsymbol{y},t)\delta t+\boldsymbol{g}\delta\boldsymbol{L})\right]|\boldsymbol{X}(t)=\boldsymbol{y}\right\}\\&=E\left\{\exp\left[\mathrm{i}\boldsymbol{k}^{\mathrm{T}}\boldsymbol{f}(\boldsymbol{y},t)\delta t+\mathrm{i}\boldsymbol{k}^{\mathrm{T}}\boldsymbol{g}\delta\boldsymbol{L}\right]|\boldsymbol{X}(t)=\boldsymbol{y}\right\}\\&=\exp\left[\mathrm{i}\boldsymbol{k}^{\mathrm{T}}\boldsymbol{f}(\boldsymbol{y},t)\delta t\right]E\left[\exp\left(\mathrm{i}\boldsymbol{k}^{\mathrm{T}}\boldsymbol{g}\delta\boldsymbol{L}\right)\right]\\&=\exp\left[\mathrm{i}\boldsymbol{k}^{\mathrm{T}}\boldsymbol{f}(\boldsymbol{y},t)\delta t\right]\exp\left[-\sum_{j=1}^{n}\delta tD_{L_j}\left|g_j\right|^{\alpha_j}\left|k_j\right|^{\alpha_j}\right].\end{aligned} \tag{7}$$

Thus, the cumulant generating function $\delta K_{\boldsymbol{X}}(\boldsymbol{k},\delta t|\boldsymbol{y},t)$ is obtained as

$$\begin{aligned}\delta K_{\boldsymbol{X}}(\boldsymbol{k},\delta t|\boldsymbol{y},t)&=\mathrm{i}\boldsymbol{k}^{\mathrm{T}}\boldsymbol{f}(\boldsymbol{y},t)\delta t-\sum_{j=1}^{n}\delta tD_{L_j}\left|g_j\right|^{\alpha_j}\left|k_j\right|^{\alpha_j}\\&=\sum_{j=1}^{n}\mathrm{i}k_jf_j(\boldsymbol{y},t)\delta t-\sum_{j=1}^{n}\delta tD_{L_j}\left|g_j\right|^{\alpha_j}\left|k_j\right|^{\alpha_j}.\end{aligned} \tag{8}$$

The inverse of the cumulant generating function is

$$\begin{aligned}&\mathcal{F}^{-1}[\delta K_{\boldsymbol{X}}(\boldsymbol{k},\delta t|\boldsymbol{y},t)]\\&=\mathcal{F}^{-1}\left[\mathrm{i}\sum_{j=1}^{n}k_jf_j(\boldsymbol{y},t)\delta t-\sum_{j=1}^{n}\delta tD_{L_j}|g_j|^{\alpha_j}|k_j|^{\alpha_j}\right]\\&=\sum_{j=1}^{n}\mathcal{F}^{-1}\left[\mathrm{i}k_j\right]f_j(\boldsymbol{y},t)\delta t-\sum_{j=1}^{n}\mathcal{F}^{-1}\left[|k_j|^{\alpha_j}\right]|g_j|^{\alpha_j}D_{L_j}\delta t\\&=-\sum_{j=1}^{n}\frac{\partial}{\partial(x_j-y_j)}\delta(\boldsymbol{x}-\boldsymbol{y})f_j(\boldsymbol{y},t)\delta t\\&\quad-\sum_{j=1}^{n}\frac{\partial^{\alpha_j}}{\partial|x_j|^{\alpha_j}}\delta(\boldsymbol{x}-\boldsymbol{y})|g_j|^{\alpha_j}D_{L_j}\delta t.\end{aligned} \tag{9}$$

Based on the inverse Fourier transformation of cumulant generating function $\mathcal{F}^{-1}[\delta K_{\boldsymbol{X}}(\boldsymbol{k},\delta t|\boldsymbol{y},t)]$, Eq. (6) can be recast into

$$\begin{aligned}&p(\boldsymbol{x},t+\delta t|\boldsymbol{x_0},t_0)-p(\boldsymbol{x},t|\boldsymbol{x_0},t_0)\\&=\int_{R^n}\int_{R^n}\frac{1}{(2\pi)^n}\exp\left[-\mathrm{i}\boldsymbol{k}^{\mathrm{T}}(\boldsymbol{x}-\boldsymbol{y})\right]\{\exp[\delta K_{\boldsymbol{X}}(\boldsymbol{k},\delta t|\boldsymbol{y},t)]-1\}\\&\quad p(\boldsymbol{y},t|\boldsymbol{x_0},t_0)\mathrm{d}\boldsymbol{k}\mathrm{d}\boldsymbol{y}\\&=\int_{R^n}\int_{R^n}\frac{1}{(2\pi)^n}\exp\left[-\mathrm{i}\boldsymbol{k}^{\mathrm{T}}(\boldsymbol{x}-\boldsymbol{y})\right]\left[\delta K_{\boldsymbol{X}}(\boldsymbol{k},\delta t|\boldsymbol{y},t)+O\left(\delta t^2\right)\right]\\&\quad p(\boldsymbol{y},t|\boldsymbol{x_0},t_0)\mathrm{d}\boldsymbol{k}\mathrm{d}\boldsymbol{y}\\&=\int_{R^n}\mathcal{F}^{-1}[\delta K_{\boldsymbol{X}}(\boldsymbol{k},\delta t|\boldsymbol{y},t)]p(\boldsymbol{y},t|\boldsymbol{x_0},t_0)\mathrm{d}\boldsymbol{y}+O\left(\delta t^2\right)\\&=\int_{R^n}\left[-\sum_{j=1}^{n}\frac{\partial}{\partial\left(x_j-y_j\right)}\delta(\boldsymbol{x}-\boldsymbol{y})f_j(\boldsymbol{y},t)\delta t\right.\\&\quad\left.-\sum_{j=1}^{n}\frac{\partial^{\alpha_j}}{\partial|x_j-y_j|^{\alpha_j}}\delta(\boldsymbol{x}-\boldsymbol{y})\left|g_j\right|^{\alpha_j}D_{L_j}\delta t\right]p(\boldsymbol{y},t|\boldsymbol{x}_0,t_0)\mathrm{d}\boldsymbol{y}\end{aligned}$$

$$= -\delta t \sum_{j=1}^{n} \frac{\partial}{\partial x_j}\left[f_j(\boldsymbol{x},t)p(\boldsymbol{x},t|\boldsymbol{x}_0,t_0)\right] + \delta t \sum_{j=1}^{n} D_{L_j}\frac{\partial^{\alpha_j}}{\partial |x_j|^{\alpha_j}}\left[\left|g_j\right|^{\alpha_j}p(\boldsymbol{x},t|\boldsymbol{x}_0,t_0)\right]. \tag{10}$$

Dividing both sides of the Eq. (10) by δt and taking the limit, we have

$$\frac{\partial}{\partial t}p(\boldsymbol{x},t|\boldsymbol{x_0},t_0) = \lim_{\delta t\to 0}\frac{p(\boldsymbol{x},t+\delta t|\boldsymbol{x_0},t_0)-p(\boldsymbol{x},t|\boldsymbol{x_0},t_0)}{\delta t} = -\sum_{j=1}^{n}\frac{\partial}{\partial x_j}\left[f_j(\boldsymbol{x},t)p(\boldsymbol{x},t|\boldsymbol{x}_0,t_0)\right] + \sum_{j=1}^{n} D_{L_j}\frac{\partial^{\alpha_j}}{\partial |x_j|^{\alpha_j}}\left[|g_j|^{\alpha_j}p(\boldsymbol{x},t|\boldsymbol{x}_0,t_0)\right], \tag{11}$$

with the initial condition

$$p(\boldsymbol{x},t|\boldsymbol{x_0},t_0) = \delta(\boldsymbol{x}-\boldsymbol{x_0}) = \prod_{j=1}^{n}\delta\left(x_j - x_{0,j}\right). \tag{12}$$

And the above fractional FPK equation (11) deduces to classical second-order FPK equation corresponding to SDE excited by Gaussian white noise when $\alpha = 2$.

Besides, the fractional operator $\partial^\alpha/\partial|x|^\alpha$ in the above derivation is the Riesz fractional derivative

$$\frac{\mathrm{d}^\alpha f(x)}{d|x|^\alpha} = \begin{cases} -\dfrac{D_+^\alpha f(x) + D_-^\alpha f(x)}{2\cos(\pi\alpha/2)}, & \alpha \neq 1 \\ -\dfrac{1}{\pi}\dfrac{\mathrm{d}}{\mathrm{d}x}\int_{-\infty}^{+\infty}\frac{f(\xi)}{x-\xi}\mathrm{d}\xi, & \alpha = 1 \end{cases}, \tag{13}$$

where

$$D_+^\alpha f(x) = \frac{1}{\Gamma(n-\alpha)}\frac{\mathrm{d}^n}{\mathrm{d}x^n}\int_{-\infty}^{x}\frac{f(\xi)}{(x-\xi)^{\alpha-n+1}}\mathrm{d}\xi, \quad D_-^\alpha f(x) = \frac{(-1)^n}{\Gamma(n-\alpha)}\frac{\mathrm{d}^n}{\mathrm{d}x^n}\int_{x}^{\infty}\frac{f(\xi)}{(\xi-x)^{\alpha-n+1}}\mathrm{d}\xi, \tag{14}$$

are the left and right Riemann-Liouville derivatives with $n = 1$ for $0 < \alpha < 1$, and $n = 2$ for $1 < \alpha \le 2$.

This part mainly presents the derivation of the path integral solution for the n-dimensional SDE under Lévy noise excitation, and its correctness is verified by proving that the corresponding fractional FPK equation is satisfied.

The transition probability density function $p(\boldsymbol{x},t+\delta t|\bar{\boldsymbol{x}},t)$, used in the path integral solution, can be obtained through the SDE (1). Taking the trajectories starting from the point $\bar{\boldsymbol{x}}$ from the whole trajectories of the response processes $\boldsymbol{X}(t)$. The trajectories (labelled as $\bar{\boldsymbol{X}}(\rho)$) between $[t, t+\delta t]$ satisfy the following SDE

$$\begin{cases} \dot{\bar{\boldsymbol{X}}}(\rho) = \boldsymbol{f}(\bar{\boldsymbol{X}},\rho) + \boldsymbol{g}(\bar{\boldsymbol{X}},\rho)\boldsymbol{\xi}(t+\rho), \\ \bar{\boldsymbol{X}}(0) = \bar{\boldsymbol{x}}, \end{cases} \quad (0 \le \rho \le \delta t), \tag{15}$$

where $\bar{\boldsymbol{x}} = (\bar{x}_1, \bar{x}_2, \cdots, \bar{x}_n)$ is a deterministic initial condition. Therefore, the transition probability density function of Eq. (1) coincides with the unconditional probability density function of the response process $\bar{\boldsymbol{X}}(\rho)$ of Eq. (15) evaluated in δt. Namely, $p(\boldsymbol{x},t+\delta t|\bar{\boldsymbol{x}},t) = p_{\bar{\boldsymbol{X}}}(\boldsymbol{x},\delta t)$. Assuming δt is small enough, $\bar{\boldsymbol{X}}(\delta t)$ can be approximated as

$$\bar{\boldsymbol{X}}(\delta t) = \bar{\boldsymbol{x}} + \boldsymbol{f}(\bar{\boldsymbol{x}},t)\delta t + \boldsymbol{g}(\bar{\boldsymbol{x}},t)d\boldsymbol{L}(t). \tag{16}$$

Considering the independence of $L_{\alpha_j}(t)(j = 1, 2\cdots n)$, $\bar{X}_j(\delta t)(j = 1, 2, \cdots, n)$ is

$$\bar{X}_j(\delta t) = \bar{x}_j + f_j(\bar{\boldsymbol{x}},t)\delta t + g_j(\bar{\boldsymbol{x}},t)dL_{\alpha_j}(t). \tag{17}$$

For the case $g_j(\bar{\boldsymbol{x}},t) = 0$, $\bar{X}_j(\delta t) = \bar{x}_j + f_j(\bar{\boldsymbol{x}},t)\delta t$ is a deterministic value. We have

$$p_{\bar{X}_j}(x_j,\delta t) = \delta\left(x_j - \bar{x}_j - f_j(\bar{\boldsymbol{x}},t)\delta t\right). \tag{18}$$

When $g_j(\bar{\boldsymbol{x}},t) \neq 0$, due to $dL_{\alpha_j}(t) \sim S_{\alpha_j}\left(\sigma_j \delta t^{1/\alpha_j}, 0, 0\right)$, then $\bar{X}_j(\delta t) \sim S_{\alpha_j}\left(|g_j(\bar{\boldsymbol{x}},t)|\sigma_j\delta t^{1/\alpha_j}, 0, \bar{x}_j + f_j(\bar{\boldsymbol{x}},t)\delta t\right)$. Thus the probability density function is

$$p_{\overline{X}_j}\left(x_j,\delta t\right) = \mathcal{F}^{-1}\left[Z_{\overline{X}_j}\left(k_j,\delta t\right)\right] = \mathcal{F}^{-1}\left[\exp\left(\mathrm{i}k_j\left(\overline{x}_j + f_j(\overline{\boldsymbol{x}},t)\delta t\right) - \delta t D_{L_j}\left|g_j(\overline{\boldsymbol{x}},t)\right|^{\alpha_j}\left|k_j\right|^{\alpha_j}\right)\right]. \tag{19}$$

To obtain the path integral solution of the SDE (1), we need to specify the matrix $\boldsymbol{g}(\boldsymbol{X},t)$. Considering the independence of $L_{\alpha_j}(t)(j = 1, 2\cdots, n)$, we can always assume that the first $r(r < n)$ values of $\boldsymbol{g}(\boldsymbol{X},t)$ are zero and the others are nonzero. Namely, $\boldsymbol{g}(\boldsymbol{X},t) = \mathrm{diag}(0,\cdots,0,g_{r+1}(\boldsymbol{X},t), g_{r+2}(\boldsymbol{X},t)\cdots, g_n(\boldsymbol{X},t))$ with $g_i(\boldsymbol{X},t) \neq 0 (i = r+1,\cdots,n)$. Then the transition probability density function can be obtained as

$$p(\boldsymbol{x},t+\delta t|\overline{\boldsymbol{x}},t) = p_{\overline{\boldsymbol{X}}}(\boldsymbol{x},\delta t) = \prod_{j=1}^{n}p_{\overline{X}_j}\left(x_j,\delta t\right) = \prod_{j=1}^{r}\delta\left(x_j - \overline{x}_j - f_j(\overline{\boldsymbol{x}},t)\delta t\right)\prod_{j=r+1}^{n}\mathcal{F}^{-1}\left[Z_{\overline{X}_j}\left(k_j,\delta t\right)\right] = \prod_{j=r+1}^{n}\mathcal{F}^{-1}\left[\exp\left(\mathrm{i}k_j\left(\overline{x}_j + f_j(\overline{\boldsymbol{x}},t)\delta t\right) - \delta t D_{L_j}\left|g_j(\overline{\boldsymbol{x}},t)\right|^{\alpha_j}\left|k_j\right|^{\alpha_j}\right)\right]\prod_{j=1}^{r}\delta\left(x_j - \overline{x}_j - f_j(\overline{\boldsymbol{x}},t)\delta t\right). \tag{20}$$

Letting $n = 1, r = 0$, the above formula reduces to the short-time transition probability density function of the one-dimensional SDE. And it degenerate into the SDOF case when $n = 2, r = 1$. Especially, when $\alpha = 2$ the above transition probability density function can be explicitly integrated as

$$p(\boldsymbol{x},t+\delta t|\overline{\boldsymbol{x}},t) = \prod_{j=r+1}^{n}\frac{1}{2\sqrt{\pi\delta t D_L}\left|g_j(\overline{\boldsymbol{x}},t)\right|}\exp\left[-\frac{\left(-x+\overline{x}+f_j(\overline{\boldsymbol{x}},t)\delta t\right)^2}{4\delta t D_L\left|g_j(\overline{\boldsymbol{x}},t)\right|^2}\right]\prod_{j=1}^{r}\delta\left(x_j - \overline{x}_j - f_j(\overline{\boldsymbol{x}},t)\delta t\right). \tag{21}$$

After getting the transition probability density function, the path integral solution can be easily obtained by the CKS equation $p(\boldsymbol{x},t+\delta t) = \int_{R^n}p(\boldsymbol{x},t+\delta t|\overline{\boldsymbol{x}},t)p(\overline{\boldsymbol{x}},t)\mathrm{d}\overline{\boldsymbol{x}}$, in which $p(\boldsymbol{x},t+\delta t|\overline{\boldsymbol{x}},t)$ is shown in formula (20). Starting from the known initial probability density function $p(\boldsymbol{x},t_0)$, we get the probability density function $p(\boldsymbol{x},t_1)$ at the next time instant $t_1 = t_0 + \delta t$. Then the probability density function $p(\boldsymbol{x},t_2), p(\boldsymbol{x},t_3),\cdots$ are obtained by recursively invoking the CKS equation until a time t that we want. Dividing the time interval $[t_0, t]$ into N parts, with the time step $\delta t = (t-t_0)/N$. Then, starting from the initial probability density function $p(\boldsymbol{x}_0,t_0)$, the probability density function $p(\boldsymbol{x},t)$ can be calculated by

$$p(\boldsymbol{x},t) = \int_{R^n}p\left(\boldsymbol{x},t\left|\boldsymbol{x}^{N-1},t_{N-1}\right.\right)\int_{R^n}p\left(\boldsymbol{x}^{N-1},t_{N-1}\left|\boldsymbol{x}^{N-2},t_{N-2}\right.\right)\cdots\int_{R^n}p\left(\boldsymbol{x}^2,t_2|\boldsymbol{x}^1,t_1\right)\int_{R^n}p\left(\boldsymbol{x}^1,t_1|\boldsymbol{x}^0,t_0\right)p(\boldsymbol{x}_0,t_0)\,\mathrm{d}\boldsymbol{x}^0\mathrm{d}\boldsymbol{x}^1\cdots\mathrm{d}\boldsymbol{x}^{N-2}\mathrm{d}\boldsymbol{x}^{N-1}. \tag{22}$$

where $t_0 < t_1 < \cdots < t_N = t, t_n = t_0 + n\delta t \quad (n = 0,1,\cdots,N)$ and $\boldsymbol{x}^n = \boldsymbol{x}(t_n)$.

The path integral solution is just the solution of the FPK equation. Although we did not directly derive the path integral solution

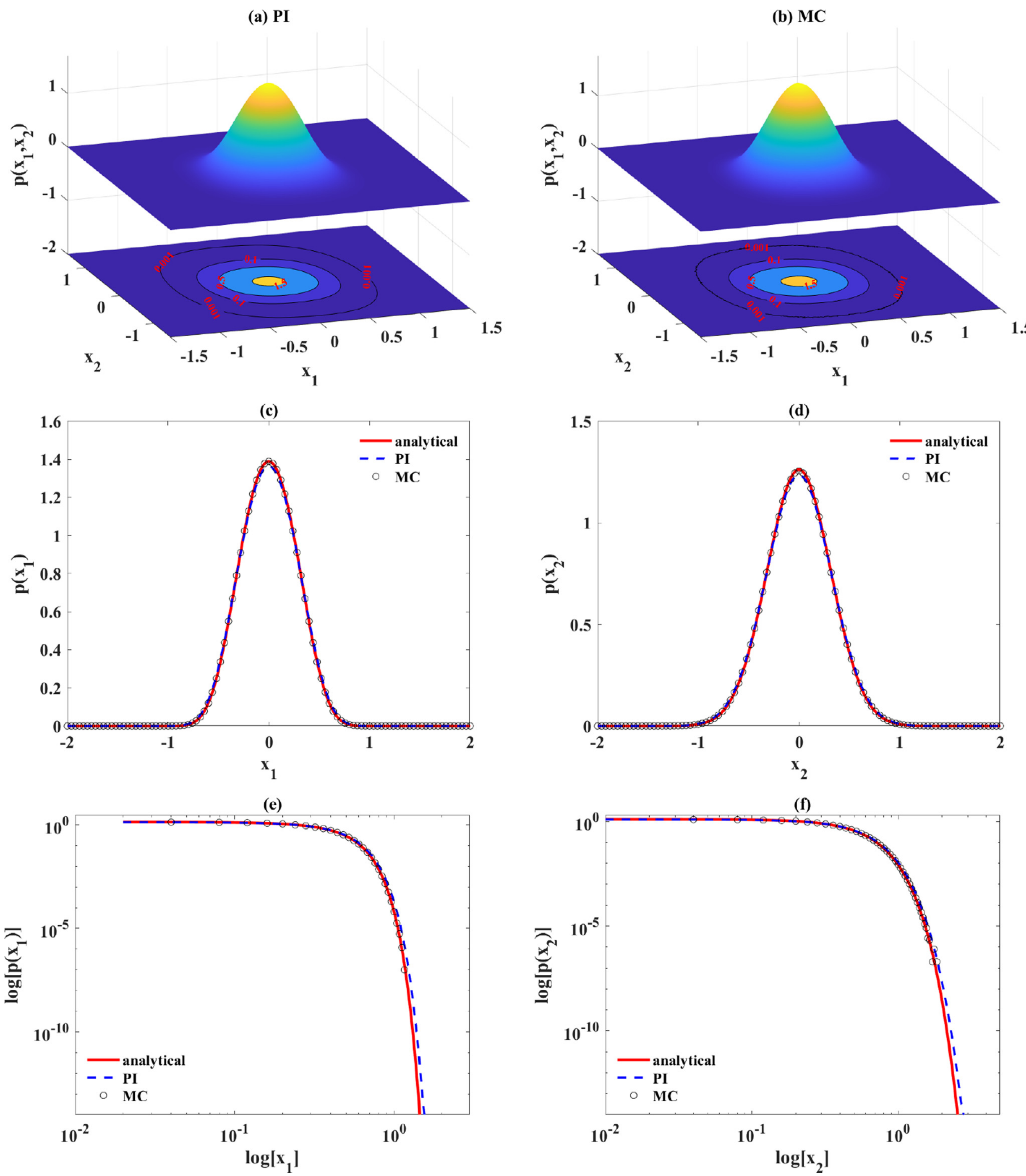

Fig. 1. Probability density functions for the system (35) when $\beta = 1, \omega_0 = -1, \delta = 2, D_L = 0.1$ and $\alpha = 2.0$. (**a**),(**b**) are the stationary joint probability density functions. (**c**),(**d**) are stationary marginal probability density functions comparison with the analytical solutions, and (**e**),(**f**) are their corresponding log-log plots.

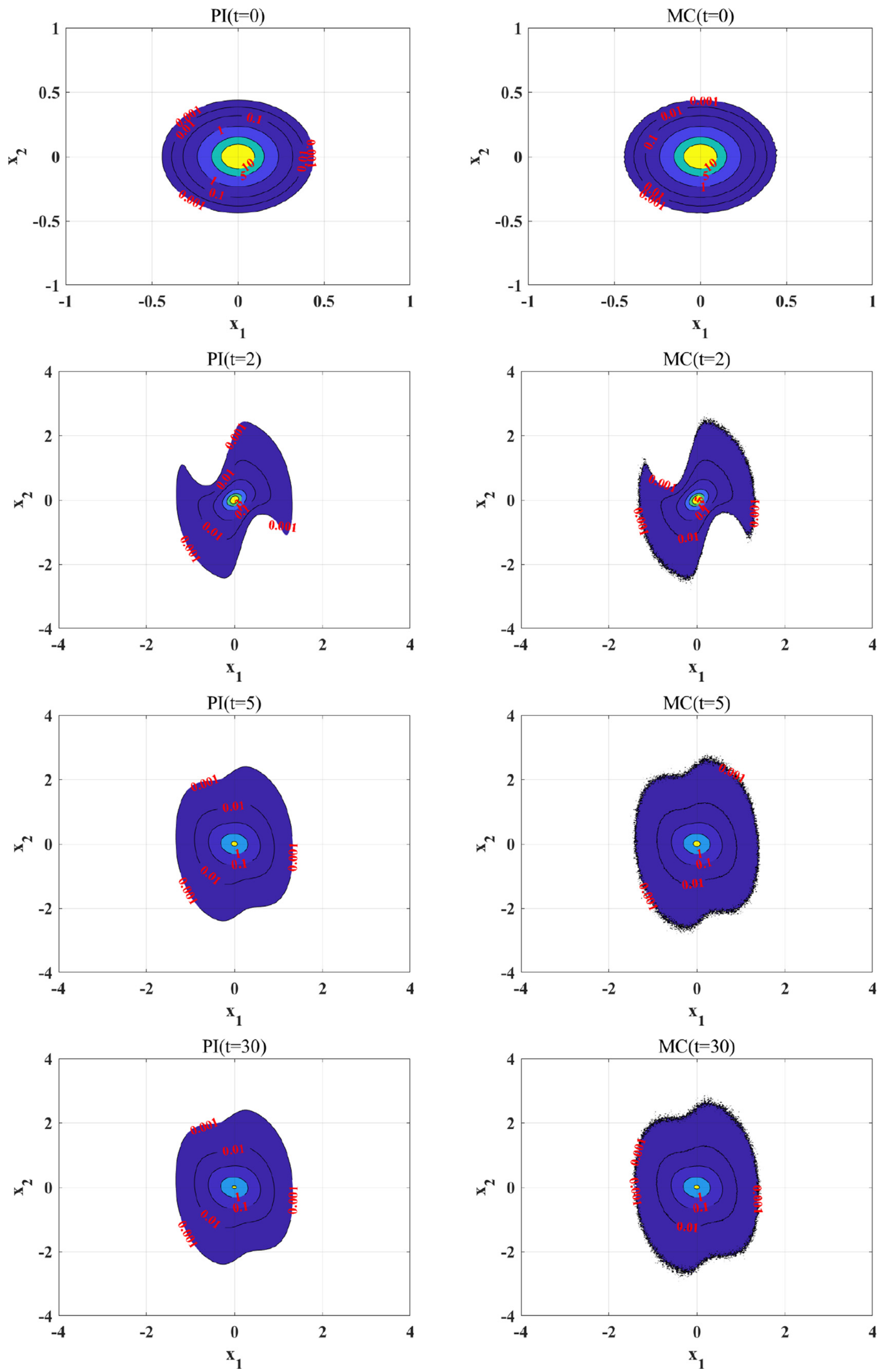

Fig. 2. Probability density functions for the system (35) when $\beta = 1, \omega_0 = -1, \delta = 2, D_L = 0.1$ and $\alpha = 1.5$.

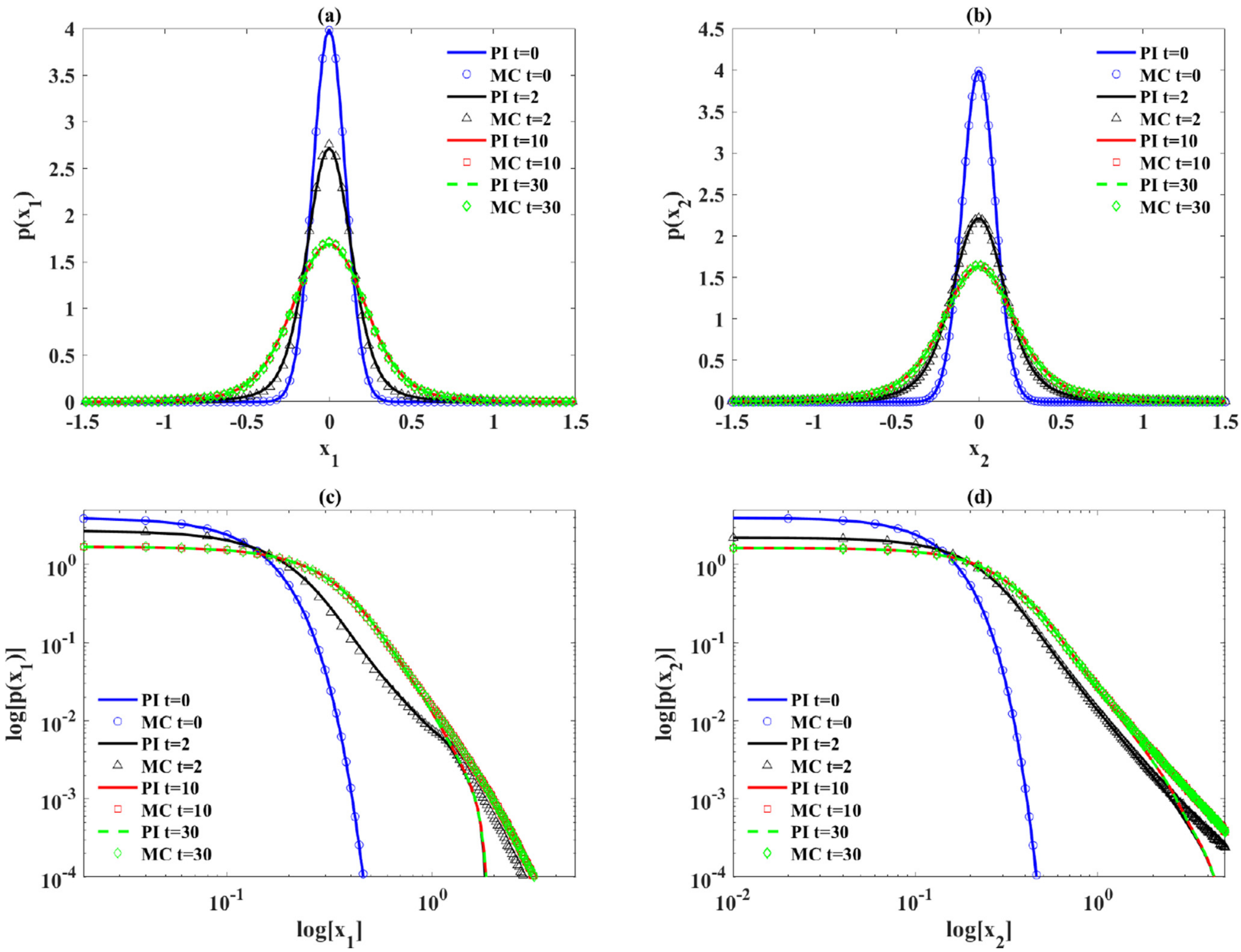

Fig. 3. Marginal probability density functions for the system (35) when $\beta = 1, \omega_0 = -1, \delta = 2, D_L = 0.1$ and $\alpha = 1.5$. (**a**),(**b**) are for x_1 and x_2, and (**c**),(**d**) are their corresponding log-log plots.

from the FPK equation, we can verify its correctness by proving that the path integral solution satisfies the FPK equation

$$\frac{\partial}{\partial t}p(\boldsymbol{x}, t|\boldsymbol{x}_0, t_0) = -\sum_{j=1}^{n}\frac{\partial}{\partial x_j}\left[f_j(\boldsymbol{x}, t)p(\boldsymbol{x}, t|\boldsymbol{x}_0, t_0)\right] + \sum_{j=r+1}^{n} D_{L_j}\frac{\partial^{\alpha_j}}{\partial |x_j|^{\alpha_j}}\left[|g_j|^{\alpha_j}p(\boldsymbol{x}, t|\boldsymbol{x}_0, t_0)\right]. \tag{23}$$

The above equation is obtained through the fractional FPK Eq. (11) by specifying the matrix $\boldsymbol{g}(\boldsymbol{X}, t) = \mathrm{diag}(0, \cdots, 0, g_{r+1}(\boldsymbol{X}, t), g_{r+2}(\boldsymbol{X}, t) \cdots, g_n(\boldsymbol{X}, t))$ with $g_i(\boldsymbol{X}, t) \neq 0 (i = r+1, \cdots, n)$.

For the sake of simplicity, the proof is performed in Fourier space to avoid directly dealing with the intractable fractional-order derivatives. The characteristic function of the path integral solution in Fourier space can be rewritten as

$$\begin{aligned} Z_{\boldsymbol{X}}(\boldsymbol{k}, t+\delta t) &= \mathcal{F}[p(\boldsymbol{x}, t+\delta t)] \\ &= \int_{R^n}\mathcal{F}[p(\boldsymbol{x}, t+\delta t|\bar{\boldsymbol{x}}, t)]p(\bar{\boldsymbol{x}}, t)\mathrm{d}\bar{\boldsymbol{x}} \\ &= \int_{R^n}\left\{\prod_{j=1}^{r}\exp\left[\mathrm{i}k_j\left(\bar{x}_j + f_j(\bar{\boldsymbol{x}}, t)\delta t\right)\right]\right. \\ &\quad \left.\prod_{j=r+1}^{n}\exp\left(\mathrm{i}k_j\left(\bar{x}_j + f_j(\bar{\boldsymbol{x}}, t)\delta t\right) - \delta t D_{L_j}\left|g_j(\bar{\boldsymbol{x}}, t)\right|^{\alpha_j}\left|k_j\right|^{\alpha_j}\right)\right\}p(\bar{\boldsymbol{x}}, t)\mathrm{d}\bar{\boldsymbol{x}} \\ &= \int_{R^n}\prod_{j=1}^{n}\exp\left[\mathrm{i}k_j\bar{x}_j\right]\prod_{j=1}^{n}\exp\left[\mathrm{i}k_j f_j(\bar{\boldsymbol{x}}, t)\delta t\right] \\ &\quad \prod_{j=r+1}^{n}\exp\left(-\delta t D_{L_j}\left|g_j(\bar{\boldsymbol{x}}, t)\right|^{\alpha_j}\left|k_j\right|^{\alpha_j}\right)p(\bar{\boldsymbol{x}}, t)\mathrm{d}\bar{\boldsymbol{x}} \\ &= \int_{R^n}\exp\left[-\mathrm{i}\boldsymbol{k}^{\mathrm{T}}\bar{\boldsymbol{x}}\right]\left\{1 + \sum_{j=1}^{n}\mathrm{i}k_j f_j(\bar{\boldsymbol{x}}, t)\delta t\right. \\ &\quad \left. - \sum_{j=r+1}^{n}D_{L_j}\left|g_j(\bar{\boldsymbol{x}}, t)\right|^{\alpha_j}\left|k_j\right|^{\alpha_j}\delta t + O\left(\delta t^2\right)\right\}p(\bar{\boldsymbol{x}}, t)\mathrm{d}\bar{\boldsymbol{x}} \\ &= Z_{\boldsymbol{X}}(\boldsymbol{k}, t) - \delta t\sum_{j=1}^{n}\mathcal{F}\left[\frac{\partial}{\partial x_j}\left(f_j(\boldsymbol{x}, t)p(\boldsymbol{x}, t)\right)\right] \\ &\quad + \delta t\sum_{j=r+1}^{n}D_{L_j}\mathcal{F}\left[\frac{\partial^{\alpha_j}}{\partial |x_j|^{\alpha_j}}\left(|g_j(\boldsymbol{x}, t)|^{\alpha_j}p(\boldsymbol{x}, t)\right)\right] + O\left(\delta t^2\right). \end{aligned} \tag{24}$$

The inverse Fourier transformation of the above equation is

$$\begin{aligned} p(\boldsymbol{x}, t+\delta t) &= p(\boldsymbol{x}, t) - \delta t\sum_{j=1}^{n}\frac{\partial}{\partial x_j}\left(f_j(\boldsymbol{x}, t)p(\boldsymbol{x}, t)\right) \\ &\quad + \delta t\sum_{j=r+1}^{n}D_{L_j}\frac{\partial^{\alpha_j}}{\partial |x_j|^{\alpha_j}}\left(|g_j(\boldsymbol{x}, t)|^{\alpha_j}p(\boldsymbol{x}, t)\right) + O(\delta t^2). \end{aligned} \tag{25}$$

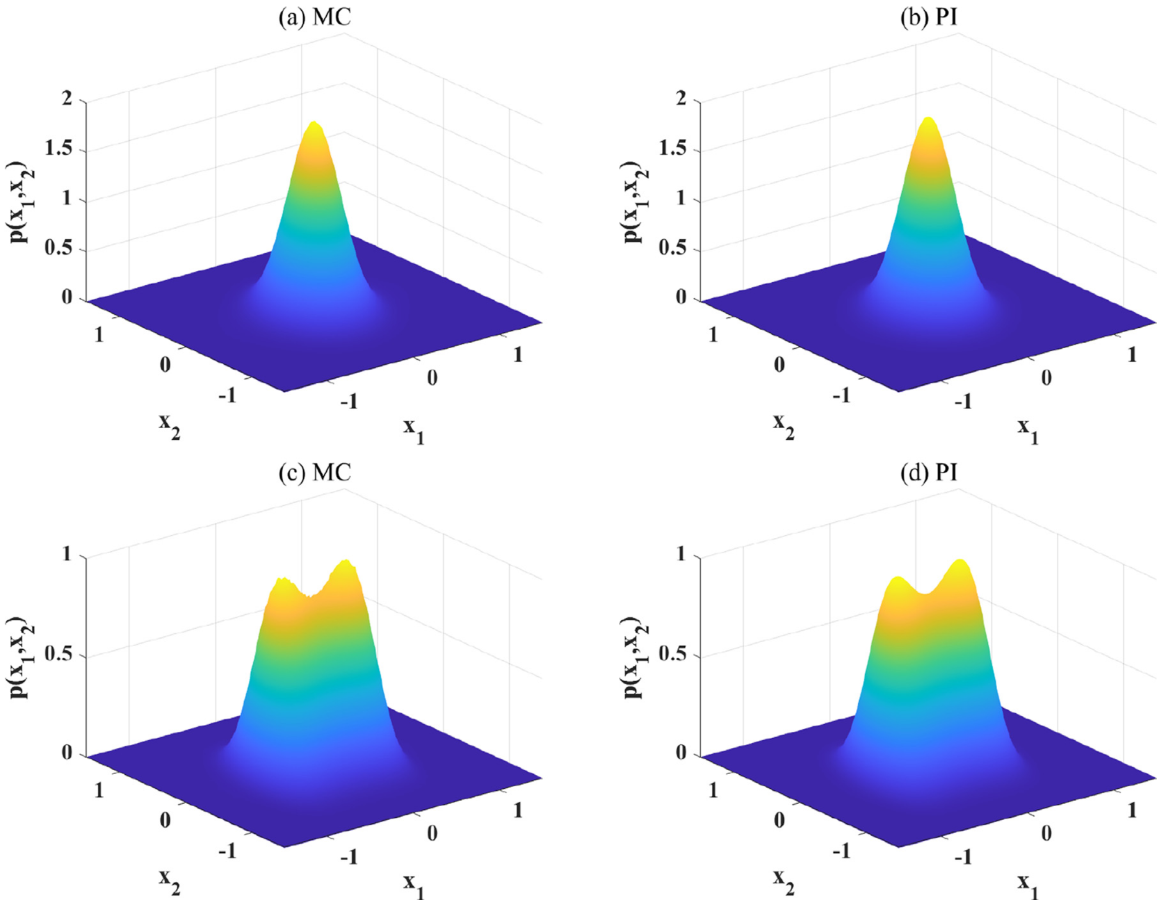

Fig. 4. Stationary probability density functions for the system (40). (**a**),(**b**) are for $f(x) = -0.5x$, $h(x) = \sqrt{1+0.1x}$, (**c**),(**d**) are for $f(x) = 0.1x - x^3$, $h(x) = \sqrt{1+0.1x}$, and other parameters are $\tau = 0.2$, $D_L = D = 0.02$, $\alpha = 1.8$.

Reshaping Eq. (25) and taking the limit $\delta t \to 0$, we get

$$\frac{\partial}{\partial t} p(\boldsymbol{x}, t) = -\sum_{j=1}^{n} \frac{\partial}{\partial x_j}\left[f_j(\boldsymbol{x}, t) p(\boldsymbol{x}, t)\right] + \sum_{j=r+1}^{n} D_{L_j} \frac{\partial^{\alpha_j}}{\partial |x_j|^{\alpha_j}}\left[|g_j|^{\alpha_j} p(\boldsymbol{x}, t)\right]. \tag{26}$$

Considering the initial condition $\boldsymbol{X}(t) = \boldsymbol{x}_0$, the FPK equation can be rewritten as Eq. (23).

According to the path integral theory, for any n-dimensional SDE, we need to perform the following two steps to obtain the path integral solution. First, the corresponding short-time transition probability density function $p(\boldsymbol{x}, t+\delta t|\bar{\boldsymbol{x}}, t)$ is derived from the SDE, where the derivation of the short-time transition probability density function is obvious according to previous discussion. And then starting from the initial conditions, the short-time transition probability density function is used for the step-by-step iteration of the CKS equation to get the path integral solution at each moment. Without any tricks, the one-step iterative formula can be numerically implemented as follows:

$$\begin{aligned} p(\boldsymbol{x}, t+\delta t) &= \int_{R^n} p(\boldsymbol{x}, t+\delta t|\bar{\boldsymbol{x}}, t) p(\bar{\boldsymbol{x}}, t) \mathrm{d}\bar{\boldsymbol{x}} \\ &= \int_{-\infty}^{+\infty}\int_{-\infty}^{+\infty}\cdots\int_{-\infty}^{+\infty} p(\boldsymbol{x}, t+\delta t|\bar{\boldsymbol{x}}, t) p(\bar{\boldsymbol{x}}, t) \mathrm{d}\bar{x}_1 \mathrm{d}\bar{x}_2 \cdots \mathrm{d}\bar{x}_n \\ &= \sum_{i_1=-N_1}^{N_1}\sum_{i_2=-N_2}^{N_2}\cdots\sum_{i_n=-N_n}^{N_n} p\left(\boldsymbol{x}, t+\delta t\left|\bar{x}_{1,i_1}, \bar{x}_{2,i_2}, \cdots, \bar{x}_{n,i_n}, t\right.\right) \\ &\quad \cdots p\left(\bar{x}_{1,i_1}, \bar{x}_{2,i_2}, \cdots, \bar{x}_{n,i_n}, t\right) \Delta\bar{x}_1 \Delta\bar{x}_2 \cdots \Delta\bar{x}_n, \end{aligned} \tag{27}$$

where $2N_k (k = 1, 2, 3, \cdots, n)$ is the number of grids divided in the x_k direction, and Δx_k is the grid size. Considering the same discretization at time t and $t + \delta t$, the one-step transition matrix, whose elements are $p(x_{1,j_1}, x_{2,j_2}, \cdots, x_{n,j_n}, t + \delta t|\bar{x}_{1,i_1}, \bar{x}_{2,i_2}, \cdots, \bar{x}_{n,i_n}, t)(-N_k \le i_k, j_k \le N_k, k = 1, 2, \cdots n)$, has a dimension of $(2N_1 \times 2N_2 \cdots \times 2N_n)^2$. It can be seen that the iteration of path integral solution leads to the curse of dimensionality as the dimension increases. The path integral method for one-dimensional examples is clearly valid and well studied, and we also experimented with SDOF systems and got some convincing results. In this section, we mainly focused on the two-dimensional and three-dimensional examples, where some tricks are used to address storage and computation issues. The path integral solutions in figures are marked with PI. To verify the correctness, the Monte Carlo solutions are calculated as a comparison, and marked with MC in the figures.

The SDOF systems with α-stable Lévy white noise can be modelled by the following SDE

$$\begin{cases} \ddot{X} + f\left(X, \dot{X}\right) = \xi_\alpha(t), \\ X(0) = X_0, \dot{X}(0) = \dot{X}_0. \end{cases} \tag{28}$$

In the above, $f\left(X, \dot{X}\right)$ is a nonlinear function of X and $\dot{X}$. And, $\xi_\alpha(t)$ is α-stable Lévy white noise with the characteristic function $Z(k) = \exp\left(-D_L|k|^\alpha\right)$, where D_L and α are the noise intensity and the stability index of the α-stable Lévy white noise, respectively. $\xi_\alpha(t)$ is the formal time derivative of a symmetric Lévy stable processes $L_\alpha(t)$.

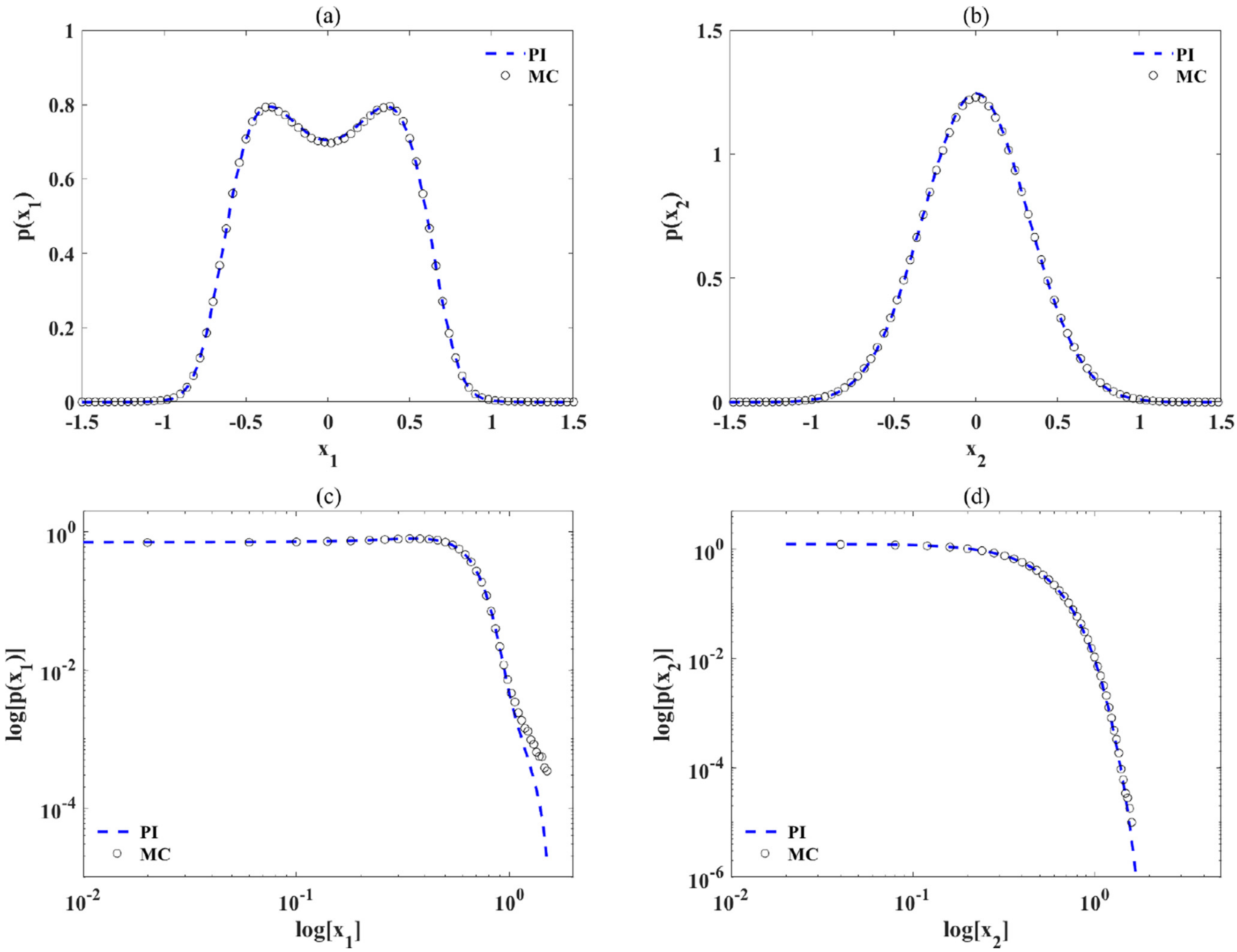

Fig. 5. Marginal stationary probability density functions for the system (40) when $f(x) = 0.1x - x^3$, $h(x) = \sqrt{1 + 0.1x}$, $\tau = 0.2$, $D_L = D = 0.02$ and $\alpha = 1.8$. (**a**),(**b**) are for x_1 and x_2, and (**c**),(**d**) are their corresponding log-log plots.

Letting $\boldsymbol{X} = [X, \dot{X}]^{\mathrm{T}} = [X_1, X_2]^{\mathrm{T}}$, then Eq. (28) can be rewritten in vector form as Eq. (1)

$$\left\{\dot{\boldsymbol{X}} = \boldsymbol{f}(\boldsymbol{X}) + \boldsymbol{g}\boldsymbol{\xi}(t), \boldsymbol{X}(0) = \boldsymbol{X}_0,\right. \tag{29}$$

where $\boldsymbol{f}(\boldsymbol{X}) = \begin{bmatrix} f_1(X_1, X_2) \\ f_2(X_1, X_2) \end{bmatrix} = \begin{bmatrix} X_2 \\ -f(X_1, X_2) \end{bmatrix}$, $\boldsymbol{g} = \begin{bmatrix} 0 & 0 \\ 0 & 1 \end{bmatrix}$, $\boldsymbol{\xi}(t) = \begin{bmatrix} 0 \\ \xi_\alpha(t) \end{bmatrix}$ and $\boldsymbol{X}_0 = \begin{bmatrix} X_0 \\ \dot{X}_0 \end{bmatrix}$. And, with $n = 2$, $r = 1$, the corresponding FPK equation is

$$\begin{aligned}\frac{\partial}{\partial t} p(x_1, x_2, t) &= -\frac{\partial}{\partial x_1}[x_2 p(x_1, x_2, t)] \\ &+ \frac{\partial}{\partial x_2}[f(x_1, x_2, t) p(x_1, x_2, t)] + D_L \frac{\partial^\alpha}{\partial |x_2|^\alpha} p(x_1, x_2, t),\end{aligned} \tag{30}$$

with the deterministic initial condition $p(x_1, x_2, 0) = \delta(x_1 - X_0)\delta(x_2 - \dot{X}_0)$ or any assigned distribution. Starting from the initial condition, the path integral solution $p(x_1, x_2, t)$ can be obtained through the formula (22), among which the short time transition probability density function is specified according to Eq. (20) as

$$\begin{aligned}p\left(x_1^n, x_2^n, t_n | x_1^{n-1}, x_2^{n-1}, t_{n-1}\right) &= \frac{\delta\left(x_1^n - x_1^{n-1} - x_2^{n-1}\delta t\right)}{2\pi} \\ \int_{-\infty}^{\infty} \exp\left(-\mathrm{i}kx_2^n\right) &\exp\left[\mathrm{i}k\left(x_2^{n-1} - f\left(x_1^{n-1}, x_2^{n-1}\right)\delta t\right) - \delta t D_L |k|^\alpha\right] \mathrm{d}k,\end{aligned} \tag{31}$$

where $t_0 < t_1 < \cdots < t_N = t, t_n = t_0 + n\delta t \ (n = 0, 1, \cdots, N)$ and $\boldsymbol{x}^n = \boldsymbol{x}(t_n) = (x_1(t_n), x_2(t_n)) = (x_1^n, x_2^n)$.

And, the probability density function $p\left(x_1^n, x_2^n, t_n\right)$ is

$$\begin{aligned}&p\left(x_1^n, x_2^n, t_n\right) \\ &= \int_{-\infty}^{\infty}\int_{-\infty}^{\infty} p\left(x_1^n, x_2^n, t_n | x_1^{n-1}, x_2^{n-1}, t_{n-1}\right) p\left(x_1^{n-1}, x_2^{n-1}, t_{n-1}\right) \mathrm{d}x_1^{n-1}\mathrm{d}x_2^{n-1} \\ &= \frac{1}{2\pi}\int_{-\infty}^{\infty}\int_{-\infty}^{\infty}\int_{-\infty}^{\infty} \delta\left(x_1^n - x_1^{n-1} - x_2^{n-1}\delta t\right) \exp\left(-\mathrm{i}kx_2^n\right)\cdots \\ &\exp\left[\mathrm{i}k\left(x_2^{n-1} - f\left(x_1^{n-1}, x_2^{n-1}\right)\delta t\right) - \delta t D_L |k|^\alpha\right] p\left(x_1^{n-1}, x_2^{n-1}, t_{n-1}\right)\mathrm{d}k\mathrm{d}x_1^{n-1}\mathrm{d}x_2^{n-1} \\ &= \frac{1}{2\pi}\int_{-\infty}^{\infty}\int_{-\infty}^{\infty} \exp\left(-\mathrm{i}kx_2^n\right)\exp\left[\mathrm{i}k\left(x_2^{n-1} - f\left(x_1^n - x_2^{n-1}\delta t, x_2^{n-1}\right)\delta t\right)\right. \\ &\quad \left.-\delta t D_L |k|^\alpha\right] p\left(x_1^n - x_2^{n-1}\delta t, x_2^{n-1}, t_{n-1}\right)\mathrm{d}k\mathrm{d}x_2^{n-1}.\end{aligned} \tag{32}$$

The above iteration can be implemented by the space partition $x_{1,i_1} = a + i_1\Delta x_1 (i_1 = 0, 1, 2, \cdots L, L = (b - a)/\Delta x_1)$ and $x_{2,i_2} = c + i_2\Delta x_2 (i_2 = 0, 1, 2, \cdots M, M = (d - c)/\Delta x_2)$ based on a finite domain $\Omega = \{(x_1, x_2) | a \le x_1 \le b, c \le x_2 \le d\}$, which is assumed to contain all the probability density functions. Then the discretized iteration formula can be rewritten as

$$\begin{aligned}&p\left(x_{1,i_1}^n, x_{2,i_2}^n, t_n\right) \\ &= \sum_{j_2=0}^{M} q\left(x_{1,i_1}^n, x_{2,i_2}^n, t_n | x_{2,j_2}^{n-1}, t_{n-1}\right) p\left(x_{1,i_1}^n - x_{2,j_2}^{n-1}\Delta t, x_{2,j_2}^{n-1}, t_{n-1}\right)\Delta x_2,\end{aligned} \tag{33}$$

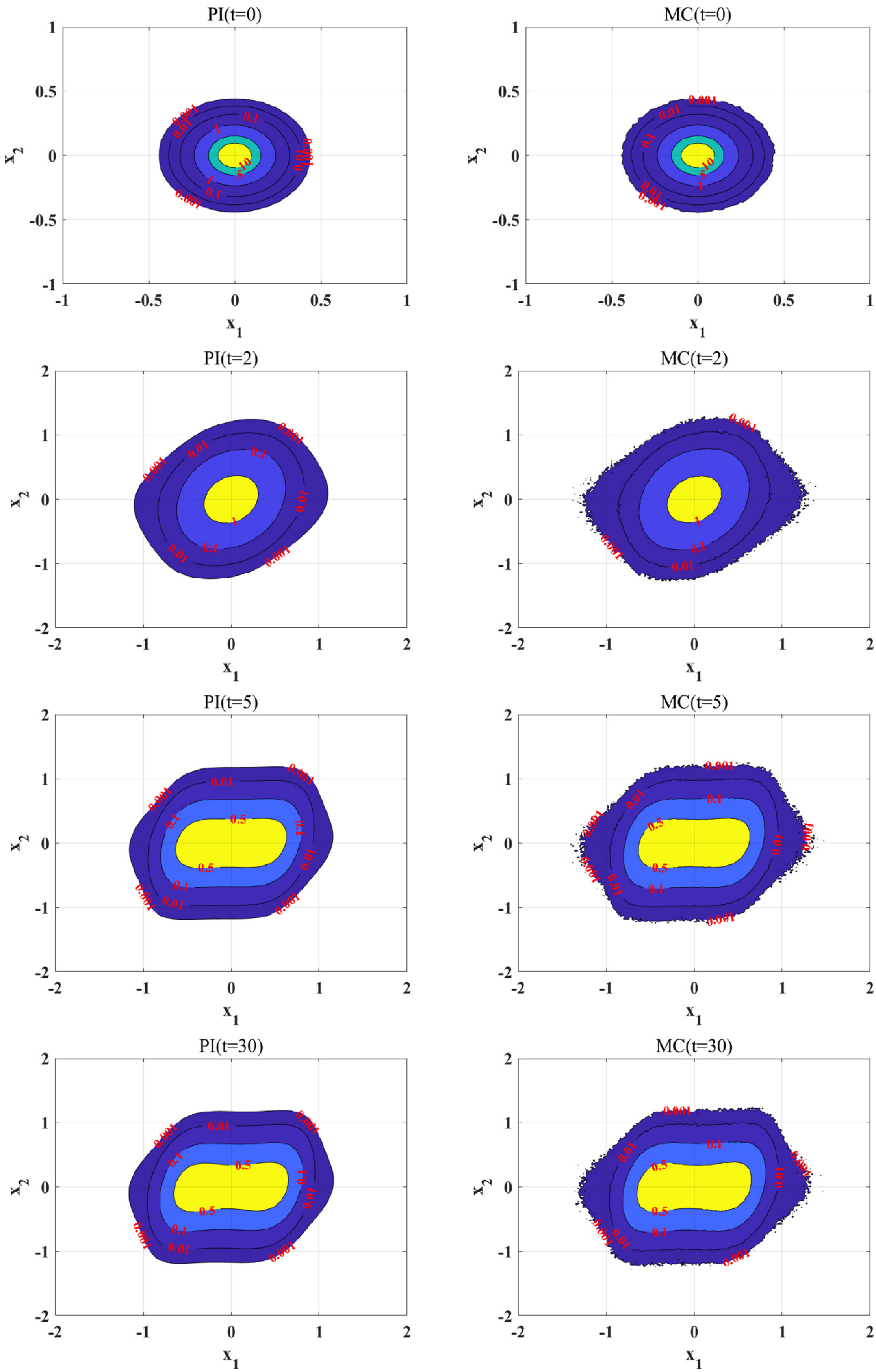

Fig. 6. Probability density functions for the system (40) when $f(x) = 0.1x - x^3$, $h(x) = \sqrt{1 + 0.1x}$, $\tau = 0.2$, $D_L = D = 0.02$ and $\alpha = 1.8$.

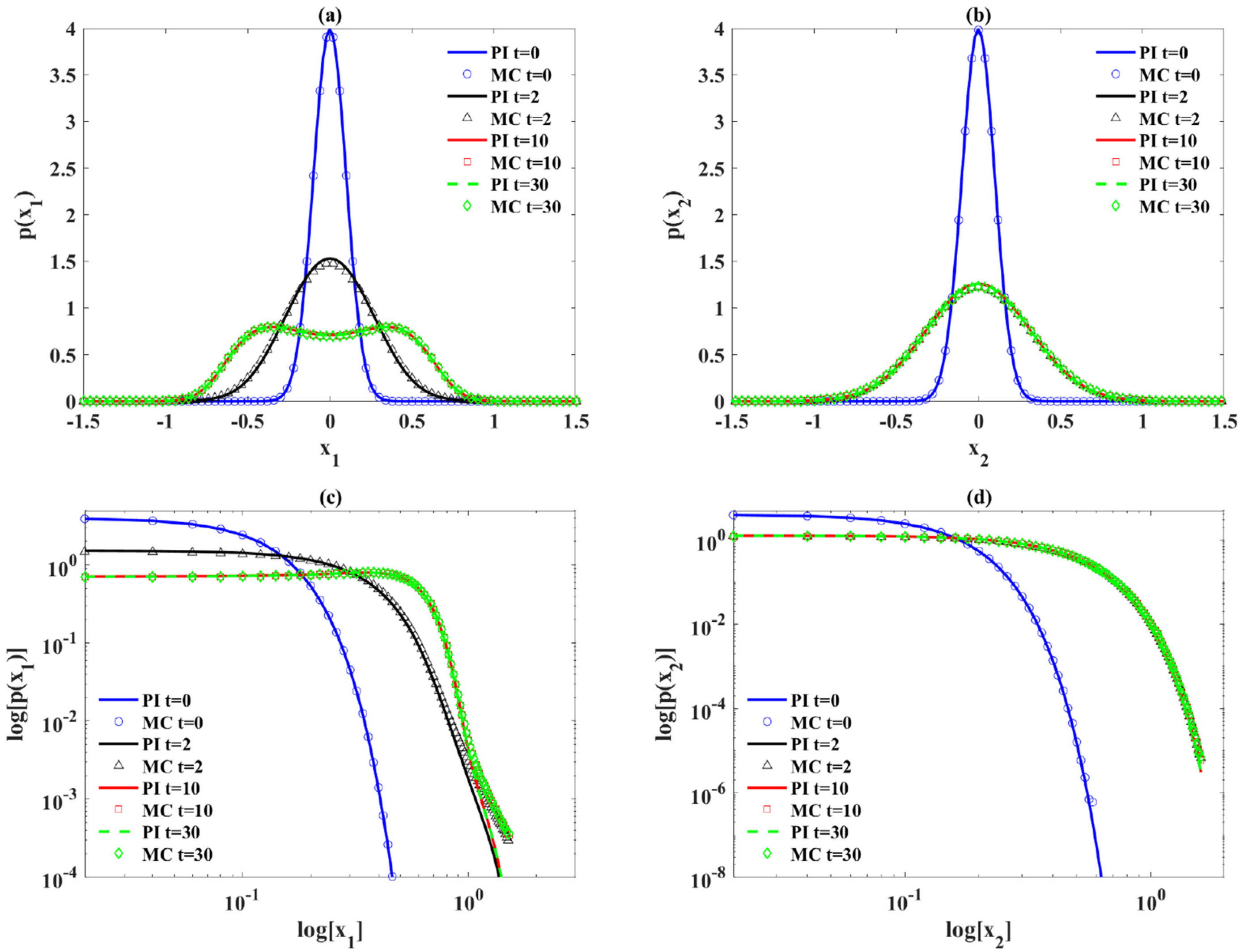

Fig. 7. Marginal probability density functions for the system (40) when $f(x) = 0.1x - x^3$, $h(x) = \sqrt{1 + 0.1x}$, $\tau = 0.2$, $D_L = D = 0.02$ and $\alpha = 1.8$. (**a**),(**b**) are for x_1 and x_2, and (**c**),(**d**) are their corresponding log-log plots.

where

$$q\left(x^n_{1,i_1}, x^n_{2,i_2}, t_n \middle| x^{n-1}_{2,j_2}, t_{n-1}\right) = \int_0^\infty \frac{1}{\pi} \exp\left[-\Delta t D_L |k|^\alpha\right]$$
$$\cos\left[k\left(-x^n_{2,i_2} + x^{n-1}_{2,j_2} - f\left(x^n_{1,i_1} - x^{n-1}_{2,i_2}\Delta t, x^{n-1}_{2,j_2}\right)\Delta t\right)\right]\mathrm{d}k, \quad (34)$$

and the value of non-grid points in the above equation can be obtained by interpolation.

Considering the Duffing oscillator with additive Lévy noise,

$$\begin{cases} \ddot{X} + \beta\dot{X} - \omega_0 X + \delta X^3 = \xi_\alpha(t), \\ X(0) = 0, \dot{X}(0) = 0, \end{cases} \quad (35)$$

whose corresponding FPK equation is (letting $\boldsymbol{X} = [X, \dot{X}]^{\mathrm{T}} = [X_1, X_2]^{\mathrm{T}}$)

$$\frac{\partial}{\partial t}p(x_1, x_2, t) = -\frac{\partial}{\partial x_1}[x_2 p(x_1, x_2, t)] + D_L\frac{\partial^\alpha}{\partial |x_2|^\alpha}p(x_1, x_2, t)$$
$$+ \frac{\partial}{\partial x_2}\left[(\beta x_2 - \omega_0 x_1 + \delta x_1^3)p(x_1, x_2, t)\right]. \quad (36)$$

When $\alpha = 2$, it has stationary solution

$$p(x_1, x_2) = \exp\left[-\frac{\beta}{2D_L}\left(x_2^2 - \omega_0 x_1^2 + \frac{\delta}{2}x_1^4\right)\right]. \quad (37)$$

For the numerical implementation, we can refer to our study of article about the path integral method of SDOF system for simplified and parallel computation of the short-time transition probability density function [22]. In the following numerical results, the spatial variables are discretized as $[-5 : 0.02 : 5] \times [-5 : 0.01 : 5]$ and time step is 0.01.

In Fig. 1, we present the path integral solution, the Monte Carlo solution and the analytical solution of system (35) at $\alpha = 2.0$. In this figure, Fig. 1a and 1b are the joint probability density functions of the system, which are displayed by surface plots and contour plots. The results show that the two numerical results fit well. Figure 1c and 1d present the marginal probability density functions of x_1 and x_2 relative to the analytical solution, and the results are well fitted. A good fit of the marginal and joint probability density functions indicates the correctness of the path integral results. In addition, Fig. 1e and 1f present log-log plots of the marginal probability density functions, Monte Carlo results with 1×10^8 sample paths calculate probability density function values as low as 1×10^{-7}, and path integral solution can be calculated even as low as 1×10^{-15}, which indicates the high precision of the path integral solution.

Figure 2 presents the transient solution of the system (35) at some moments from the initial to the stationary when $\alpha = 1.5$. Due to the lack of an analytical solution, we adopted the Monte

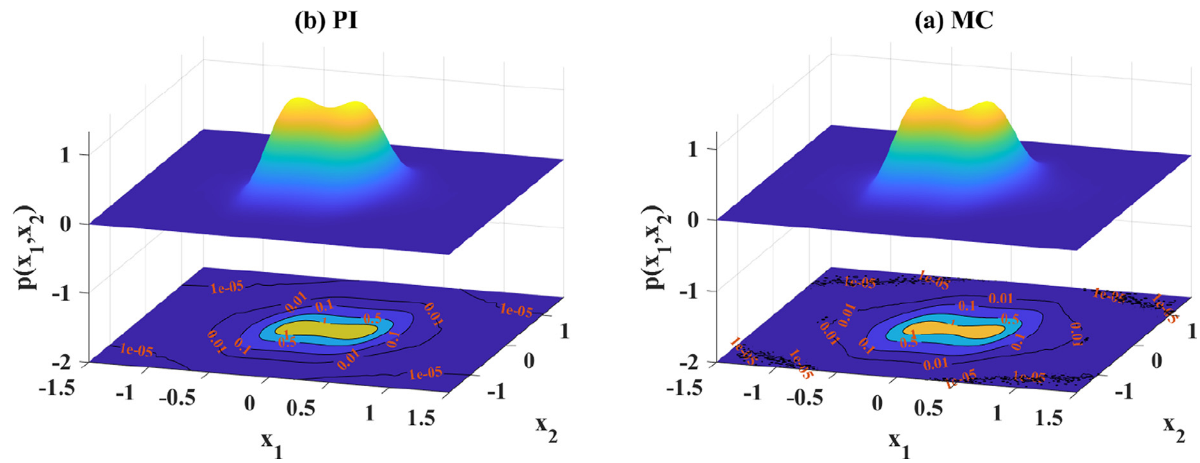

Fig. 8. Stationary probability density functions for the system (40) when $f(x)=0.01x-3x^3$, $h(x)=\sqrt{1+0.1x}$, $\tau=0.2$, $D_L=0.1$, $D=0.02$ and $\alpha=0.9$.

Carlo solution for comparison with the path integral solution. The computational cost of the path integral solutions and the Monte Carlo solutions with 1×10^8 sample paths are 4.75831×10^4 s and 2.12310×10^5 s, respectively. The contour plot of the joint probability density function of the system at time $t=0,2,5,30$ is presented. The Monte Carlo solution is consistent with the path integral solution, indicating the effectiveness of path integral method in solving the transient solution, and the same contour lines indicate that the accuracy is at least 1×10^{-3}. The marginal probability density function of the transient solution is presented in Fig. 3. The path integral solutions and the Monte Carlo solutions fit well at each moment, and their log-log plots show that the precision is higher than 10^{-3} by enlarging the tail region.

The scalar SDE with colored Gaussian parametric noise and Lévy external noise reads

$$\begin{cases}\dot{X}(t)=f(X,t)+h(X,t)\xi_c(t)+\xi_\alpha(t),\\ X(0)=x_0,\end{cases}\tag{38}$$

where $\xi_c(t)$ and $\xi_\alpha(t)$ are colored Gaussian and α-stable Lévy white noises, and both noise sources are considered to be independent from another. Moreover, $f(X,t)$ and $h(X,t)$ are functions of X and t, and x_0 is the initial value of $X(t)$ at time $t=t_0$. In the above, colored Gaussian noise is exponentially correlated with the mean value $E[\xi_c(t)]=0$ and the correlation function $R(\tau)=E[\xi_c(t)\xi_c(t')]=\frac{D}{\tau}\exp(-\frac{|t-t'|}{\tau})$. This colored Gaussian noise can be expressed by a Langevin equation

$$\dot{\xi}_c(t)=-\frac{1}{\tau}\xi_c(t)+\frac{\sqrt{2D}}{\tau}\xi(t),\tag{39}$$

where $\xi(t)$ is standard Gaussian white noise.

Letting $\boldsymbol{X}=[X,\xi_c]^{\mathrm{T}}=[X_1,X_2]^{\mathrm{T}}$, Eq. (38) can be rewritten as

$$\begin{cases}\dot{X}_1=f(X_1,X_2,t)+h(X_1,X_2,t)X_2+\xi_\alpha(t),\\ \dot{X}_2=-\frac{1}{\tau}X_2+\frac{\sqrt{2D}}{\tau}\xi(t),\end{cases}\tag{40}$$

with the initial condition

$$\begin{cases}X_1(0)=X(0)=x_0,\\ X_2(0)=\xi_c(0)=\xi_{c0},\end{cases}\tag{41}$$

where ξ_{c0} is a random variable with given probability density function. And this equation can be written in vector form as

$$\begin{cases}\dot{\boldsymbol{X}}(t)=\boldsymbol{f}(\boldsymbol{X},t)+\boldsymbol{g}(\boldsymbol{X},t)\boldsymbol{\xi}(t),\\ \boldsymbol{X}(t)=\boldsymbol{x}_0,\end{cases}\tag{42}$$

where $\boldsymbol{f}(\boldsymbol{X})=\begin{bmatrix}f(X_1,X_2,t)+h(X_1,X_2,t)X_2\\ -\frac{1}{\tau}X_2\end{bmatrix}$, $\boldsymbol{g}=\begin{bmatrix}1&0\\0&\frac{\sqrt{2D}}{\tau}\end{bmatrix}$, $\boldsymbol{\xi}(t)=\begin{bmatrix}\xi_\alpha(t)\\ \xi(t)\end{bmatrix}$ and $\boldsymbol{x}_0=\begin{bmatrix}x_0\\ \xi_{c0}\end{bmatrix}$. With $n=2$ and $r=2$, the corresponding FPK equation is

$$\begin{aligned}\frac{\partial}{\partial t}p(x_1,x_2,t)&=-\frac{\partial}{\partial x_1}[(f(x_1,x_2,t)+h(x_1,x_2,t)x_2)p(x_1,x_2,t)]\\&\quad-\frac{\partial}{\partial x_2}\left[-\frac{1}{\tau}x_2p(x_1,x_2,t)\right]+D_L\frac{\partial^\alpha}{\partial|x_1|^\alpha}[p(x_1,x_2,t)]\\&\quad+\frac{1}{2}\frac{\partial^2}{\partial|x_2|^2}\left[\frac{2D}{\tau^2}p(x_1,x_2,t)\right],\end{aligned}\tag{43}$$

with the initial condition $p(x_1,x_2,0)=p_{X_1}(x_1)p_{\xi_{c0}}(x_2)$. Starting from the initial condition, the path integral solution $p(x_1,x_2,t)$ can be obtained through the formula (22). Among which the short time transition probability density function is specified according to Eq. (20) as

$$\begin{aligned}&p\left(x_1^n,x_2^n,t_n|x_1^{n-1},x_2^{n-1},t_{n-1}\right)\\&=\mathcal{F}^{-1}\left\{\exp\left[ik_1\left(x_1^{n-1}+\left(f\left(x_1^{n-1},x_2^{n-1}\right)\right.\right.\right.\right.\\&\quad\left.\left.\left.\left.+h\left(x_1^{n-1},x_2^{n-1}\right)x_2^{n-1}\right)\delta t\right)-\delta tD_L|k_1|^\alpha\right]\right\}\\&\quad\mathcal{F}^{-1}\left\{\exp\left[ik_2\left(x_2^{n-1}-\frac{1}{\tau}x_2^{n-1}\delta t\right)-\frac{1}{2}\delta t\frac{2D}{\tau^2}|k_2|^2\right]\right\}\\&=\frac{1}{2\pi}\int_{-\infty}^{\infty}\exp\left(-ik_1x_1^n\right)^{\exp}\left[ik_1\left(x_1^{n-1}+\left(f\left(x_1^{n-1},x_2^{n-1}\right)\right.\right.\right.\\&\quad\left.\left.\left.+h\left(x_1^{n-1},x_2^{n-1}\right)x_2^{n-1}\right)\delta t\right)-\delta tD_L|k_1|^\alpha\right]dk_1\\&\quad\frac{1}{2\pi}\int_{-\infty}^{\infty}\exp\left(-ik_2x_2^n\right)\exp\left[ik_2\left(x_2^{n-1}-\frac{1}{\tau}x_2^{n-1}\delta t\right)-\delta t\frac{D}{\tau^2}|k_2|^2\right]dk_2\\&=\frac{1}{2\pi}\int_{-\infty}^{\infty}\exp\left(-ik_1x_1^n\right)\exp\left[ik_1\left(x_1^{n-1}+\left(f\left(x_1^{n-1},x_2^{n-1}\right)\right.\right.\right.\\&\quad\left.\left.\left.+h\left(x_1^{n-1},x_2^{n-1}\right)x_2^{n-1}\right)\delta t\right)-\delta tD_L|k_1|^\alpha\right]dk_1\\&\quad\frac{\tau}{\sqrt{4\pi\delta tD}}\exp\left[-\frac{\tau^2\left(-x_2^n+x_2^{n-1}-\frac{1}{\tau}x_2^{n-1}\delta t\right)^2}{4\delta tD}\right],\end{aligned}\tag{44}$$

where $t_0<t_1<\cdots<t_N=t, t_n=t_0+n\delta t$ $(n=0,1,\cdots,N)$ and $\boldsymbol{x}^n=\boldsymbol{x}(t_n)=(x_1(t_n),x_2(t_n))=(x_1^n,x_2^n)$. With this transition probability

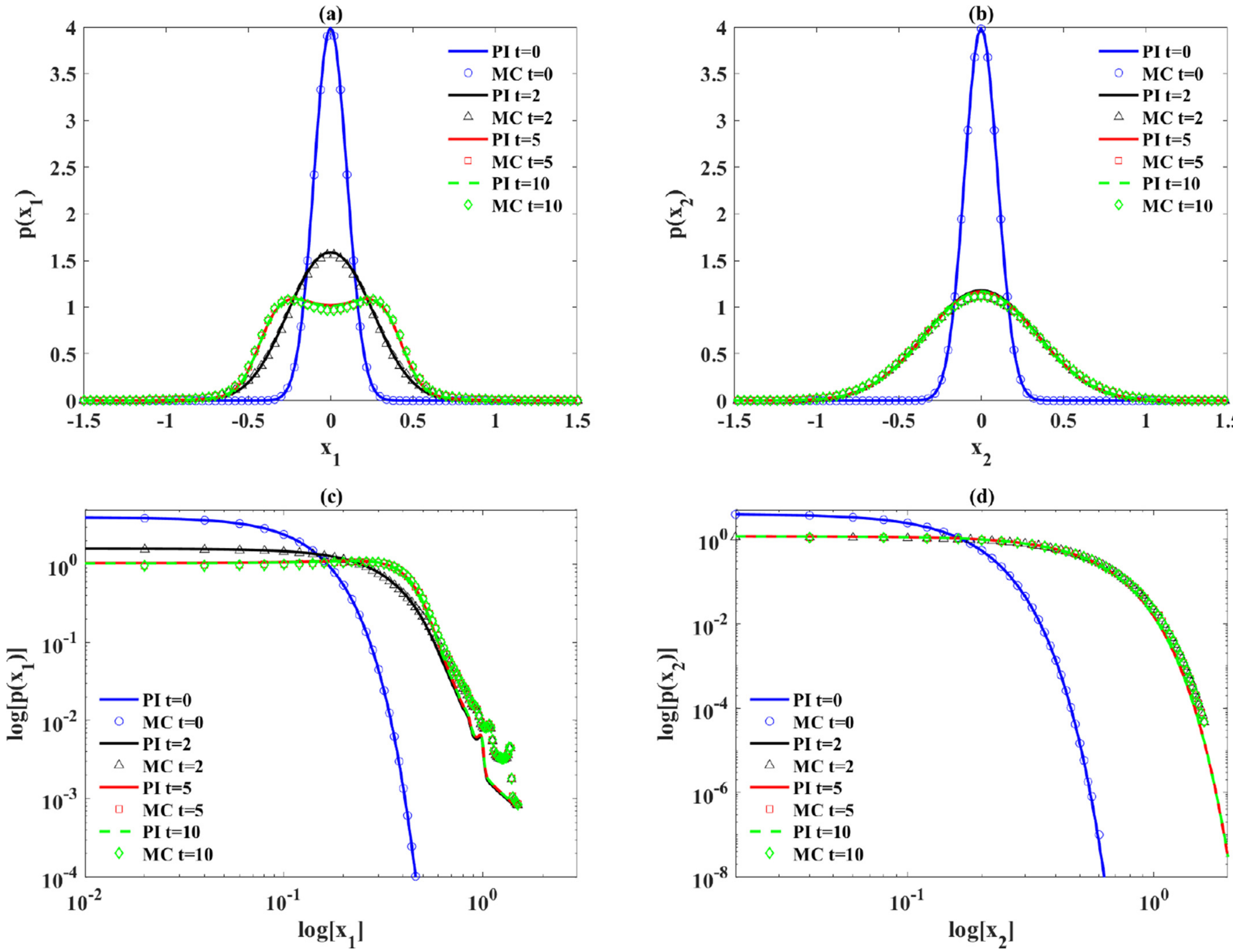

Fig. 9. Marginal probability density functions for the system (40) when $f(x) = 0.01x - 3x^3$, $h(x) = \sqrt{1 + 0.1x}$, $\tau = 0.2$, $D_L = 0.1$, $D = 0.02$ and $\alpha = 0.9$. (**a**),(**b**) are for x_1 and x_2, and (**c**),(**d**) are their corresponding log-log plots.

density function, the probability density function $p\left(x_1^n, x_2^n, t_n\right)$ can be calculated as

$$p(x_1^n, x_2^n, t_n) = \int_{-\infty}^{\infty}\int_{-\infty}^{\infty} p\left(x_1^n, x_2^n, t_n | x_1^{n-1}, x_2^{n-1}, t_{n-1}\right) p\left(x_1^{n-1}, x_2^{n-1}, t_{n-1}\right) \mathrm{d}x_1^{n-1}\mathrm{d}x_2^{n-1} = \sum_{j_1=0}^{L}\sum_{j_2=0}^{M} p\left(x_1^n, x_2^n, t_n | x_{1,j_1}^{n-1}, x_{2,j_2}^{n-1}, t_{n-1}\right) p\left(x_{1,j_1}^{n-1}, x_{2,j_2}^{n-1}, t_{n-1}\right) \Delta x_1 \Delta x_2. \tag{45}$$

Since the component x_2 is Gaussian distributed, a part of the transition probability density function can be integrated into an exponential analytical form, which reduces the one-fold integration of the transition probability density function calculation. After that, we only need to solve the problem of storage capacity of the transition matrix in numerical implementation. When implementing numerically, we perform each step of the path integral iteration by reshaping the matrix into a low-dimensional matrix, and divide the region like the SDOF system when the matrix is very large to speed up the calculation of the transition matrix.

We calculate the stationary solution of the system under two different sets of parameters and verify them with the Monte Carlo solution, which are presented in Fig. 4. In numerical implementation, the space partition is selected as $[-1.5 : 0.01 : 1.5] \times [-2 : 0.02 : 2]$ and the time-step is 0.01 for the path integral and Monte Carlo solution. The running time of the path integral solutions and the Monte Carlo solutions with 1×10^8 sample paths are $6.11112 \times 10^4 s$ and $1.89466 \times 10^5 s$, respectively. The same shape and color of the three dimensional surface plots show the correctness of the path integral solutions. Comparing the results of these two sets of parameters, the path integral method can not only capture the results of unimodal, but is also effective in the complicated bimodal case.

In Fig. 5, we also present the stationary marginal probability density functions and their log-log plots. The results show that the path integral solutions of the marginal probability density functions of x_1 and x_2 fit well with the Monte Carlo solutions with 1×10^8 sample paths. The log-log plots are also fitted, which shows that our path integral method can accurately calculate the PDF value down to around 10^{-5} by enlarging the tail region of the probability density function.

Then, in order to show the effectiveness of the path integral method for the transient solutions, we present the contour plots of the transient probability density functions of the bimodal example at $t = 0, 2, 5, 30$ in Fig. 6, and annotate the contours on the plots. The results show that the contour plot of the path integral solution and the Monte Carlo solution at each moment are consistent, indi-

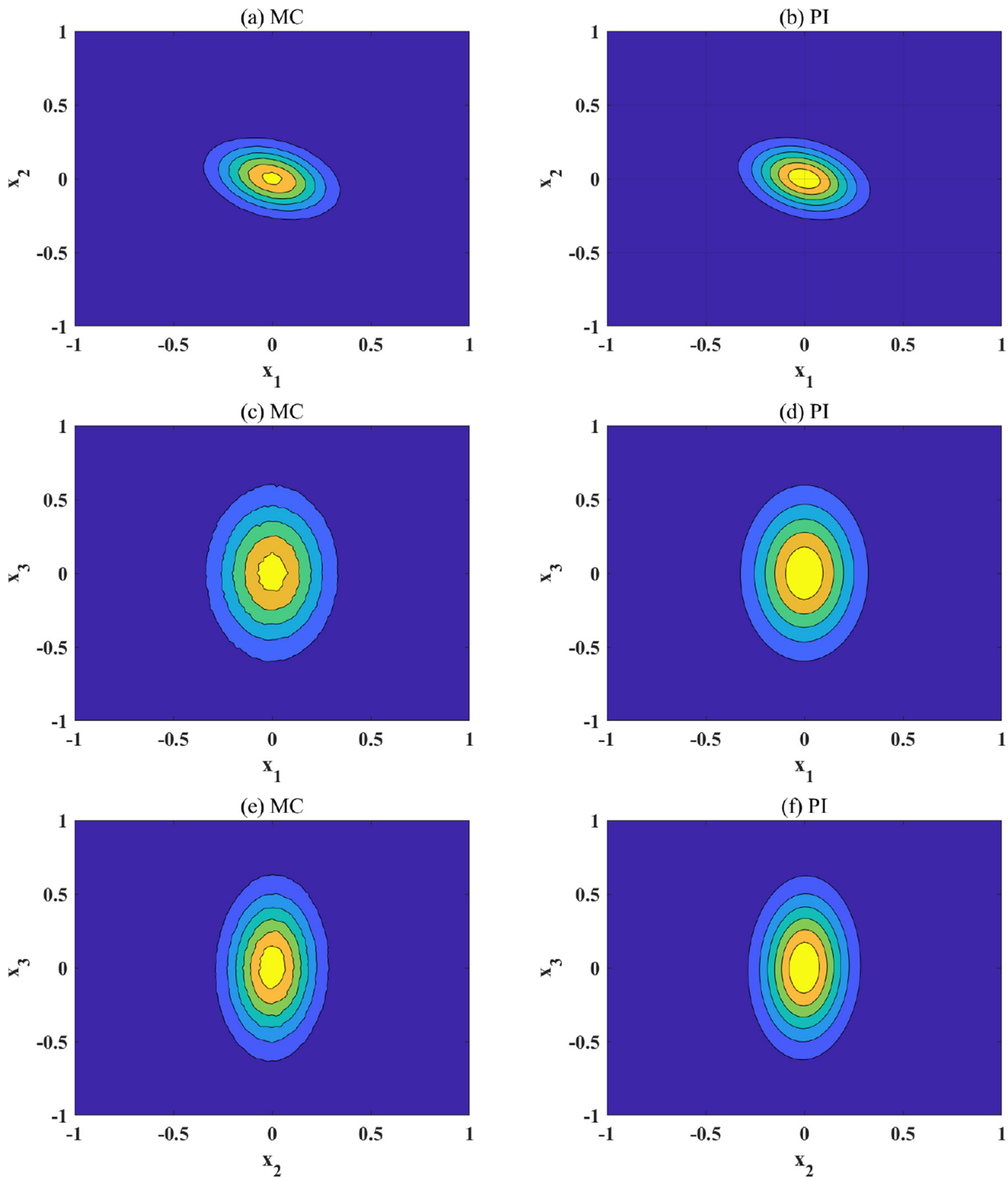

Fig. 10. Marginal joint probability density functions for the system (47) at $t = 1$ when $f(x, \dot{x}) = x - \dot{x}$, $h(x, \dot{x}) = 0.1$, $\tau = 0.2$, $D_L = 0.02$, $D = 0.02$ and $\alpha = 1.8$. (**a**),(**b**) are for $p(x_1, x_2)$, (**c**),(**d**) are for $p(x_1, x_3)$, and (**e**),(**f**) are for $p(x_2, x_3)$.

cating that the path integral method can accurately determine the transient solutions at each moment. In Fig. 7, the marginal probability density functions are presented. The probability density function of x_1 is fitted at 10^{-3} and the probability density function of x_2 is fitted at 10^{-6}, respectively.

For generality, the path integral solutions with $\alpha = 0.9$ is presented in Figs. 8 and 9. In numerical implementation, the space partition is selected as $[-1.5 : 0.01 : 1.5] \times [-1.6 : 0.02 : 1.6]$ and the time-step is 0.05 for the path integral and Monte Carlo solution. Running time of the path integral solutions and Monte Carlo solutions with 1×10^8 sample paths are 4.33232×10^4 s and 4.03310×10^4 s, respectively. The same surface plots and contour lines of the stationary joint probability density function in Fig. 8 and the good fits of the marginal probability density function in Fig. 9 show the correctness of the path integral solutions.

The second order stochastic differential equation with colored Gaussian parametric noise and Lévy external noise reads

$$\begin{cases} \ddot{X}(t) = f(X, \dot{X}, t) + h(X, \dot{X}, t)\xi_c(t) + \xi_\alpha(t), \\ X(0) = x_0, \\ \dot{X}(0) = \dot{x}_0, \end{cases} \tag{46}$$

where the definition of $\xi_c(t)$ and $\xi_\alpha(t)$ can refer to previous paragraph. $f(X, \dot{X}, t)$ and $h(X, \dot{X}, t)$ are functions of X, $\dot{X}$ and t, x_0 and $\dot{x}_0$ are the initial value of $X(t)$ and $\dot{X}(t)$ at time $t = t_0$.

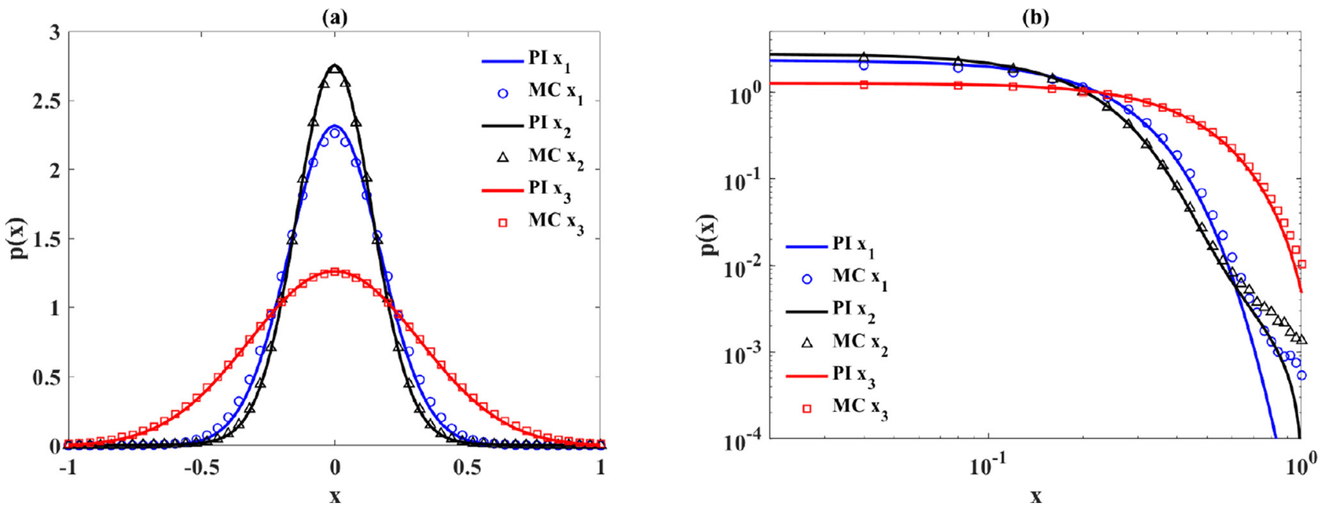

Fig. 11. Marginal probability density functions for the system (47) at $t = 1$ when $f(x, \dot{x}) = x - \dot{x}$, $h(x, \dot{x}) = 0.1$, $\tau = 0.2$, $D_L = 0.02$, $D = 0.02$ and $\alpha = 1.8$. (**a**) presents the results for x_1, x_2, x_3, and (**b**) is the corresponding log-log plot.

Letting $\boldsymbol{X} = [X, \dot{X}, \xi_c]^{\mathrm{T}} = [X_1, X_2, X_3]^{\mathrm{T}}$, Eq. (46) can be rewritten in vector form as

$$\begin{cases} \dot{\boldsymbol{X}}(t) = \boldsymbol{f}(\boldsymbol{X}, t) + \mathbf{g}(\boldsymbol{X}, t)\boldsymbol{\xi}(t), \\ \boldsymbol{X}(t) = \boldsymbol{x}_0, \end{cases} \tag{47}$$

In the above equation, $\boldsymbol{f}(\boldsymbol{X}) = \begin{bmatrix} X_2 \\ f(X_1, X_2, t) + h(X_1, X_2, t)X_3 \\ -\frac{1}{\tau}X_3 \end{bmatrix}$, $\mathbf{g}(\boldsymbol{X}) = \begin{bmatrix} 0 & 0 & 0 \\ 0 & 1 & 0 \\ 0 & 0 & \frac{\sqrt{2D}}{\tau} \end{bmatrix}$, $\boldsymbol{\xi}(t) = \begin{bmatrix} 0 \\ \xi_\alpha(t) \\ \xi(t) \end{bmatrix}$ and $\boldsymbol{x}_0 = \begin{bmatrix} x_0 \\ \dot{x}_0 \\ \xi_{c0} \end{bmatrix}$. With $n = 3$ and $r = 2$, the corresponding FPK equation is

$$\begin{aligned} &\frac{\partial}{\partial t} p(x_1, x_2, x_3, t) \\ &= -\frac{\partial}{\partial x_2}[(f(x_1, x_2, t) + h(x_1, x_2, t)x_3)p(x_1, x_2, x_3, t)] \\ &\quad - \frac{\partial}{\partial x_1}[x_2 p(x_1, x_2, x_3, t)] - \frac{\partial}{\partial x_3}\left[-\frac{1}{\tau}x_3 p(x_1, x_2, x_3, t)\right] \\ &\quad + D_L \frac{\partial^\alpha}{\partial |x_2|^\alpha}[p(x_1, x_2, x_3, t)] \\ &\quad + \frac{1}{2}\frac{\partial^2}{\partial |x_3|^2}\left[\frac{2D}{\tau^2}p(x_1, x_2, x_3, t)\right], \end{aligned} \tag{48}$$

where the initial condition $p(x_1, x_2, x_3, 0) = \delta(x_1 - x_0)\delta(x_2 - \dot{x}_0)p_{\xi_{c0}}(x_3)$. Starting from the initial condition, the path integral solution $p(x_1, x_2, x_3, t)$ can be obtained through the formula (22). Among which the short time transition probability density function is specified according to Eq. (20) as

$$\begin{aligned} &p\left(x_1^n, x_2^n, x_3^n, t_n | x_1^{n-1}, x_2^{n-1}, x_3^{n-1}, t_{n-1}\right) \\ &= \delta\left(x_1^n - x_1^{n-1} - x_2^{n-1}\delta t\right) \\ &\quad \times \mathcal{F}^{-1}\left\{\exp\left[\mathrm{i}k_2\left(x_2^{n-1} + \left(f\left(x_1^{n-1}, x_2^{n-1}\right)\right.\right.\right.\right. \\ &\quad \left.\left.\left.\left. + h\left(x_1^{n-1}, x_2^{n-1}\right)x_3^{n-1}\right)\delta t\right) - \delta t D_L |k_2|^\alpha\right]\right\} \\ &\quad \times \mathcal{F}^{-1}\left\{\exp\left[\mathrm{i}k_3\left(x_3^{n-1} - \frac{1}{\tau}x_3^{n-1}\delta t\right) - \frac{1}{2}\delta t \frac{2D}{\tau^2}|k_3|^2\right]\right\} \\ &= \delta\left(x_1^n - x_1^{n-1} - x_2^{n-1}\delta t\right) \\ &\quad \times \frac{1}{2\pi}\int_{-\infty}^{\infty} \exp\left(-\mathrm{i}k_2 x_2^n\right) \exp\left[\mathrm{i}k_2\left(x_2^{n-1} + \left(f\left(x_1^{n-1}, x_2^{n-1}\right)\right.\right.\right. \\ &\quad \left.\left.\left. + h\left(x_1^{n-1}, x_2^{n-1}\right)x_3^{n-1}\right)\delta t\right) - \delta t D_L |k_2|^\alpha\right]\mathrm{d}k_2 \\ &\quad \times \frac{\tau}{\sqrt{4\pi\delta t D}} \exp\left[-\frac{\tau^2\left(-x_3^n + x_3^{n-1} - \frac{1}{\tau}x_3^{n-1}\delta t\right)^2}{4\delta t D}\right], \end{aligned} \tag{49}$$

where $t_0 < t_1 < \cdots < t_N = t, t_n = t_0 + n\delta t \ (n = 0, 1, \cdots, N)$ and $\boldsymbol{x}^n = \boldsymbol{x}(t_n) = (x_1(t_n), x_2(t_n), x_3(t_n)) = (x_1^n, x_2^n, x_3^n)$. And, the probability density function $p\left(x_1^n, x_2^n, x_3^n, t_n\right)$ can be

$$\begin{aligned} &p(x_1^n, x_2^n, x_3^n, t_n) \\ &= \int_{-\infty}^{\infty}\int_{-\infty}^{\infty}\int_{-\infty}^{\infty} p\left(x_1^n, x_2^n, x_3^n, t_n | x_1^{n-1}, x_2^{n-1}, x_3^{n-1}, t_{n-1}\right) \\ &\quad p\left(x_1^{n-1}, x_2^{n-1}, x_3^{n-1}, t_{n-1}\right)\mathrm{d}x_1^{n-1}\mathrm{d}x_2^{n-1}\mathrm{d}x_3^{n-1} \\ &= \frac{1}{2\pi}\frac{\tau}{\sqrt{4\pi\delta t D}}\int_{-\infty}^{\infty}\int_{-\infty}^{\infty}\int_{-\infty}^{\infty} \exp\left(-\mathrm{i}k_2 x_2^n\right) \\ &\quad \times \exp\left[\mathrm{i}k_2\left(x_2^{n-1} + \left(f\left(x_1^n - x_2^{n-1}\delta t, x_2^{n-1}\right)\right.\right.\right. \\ &\quad \left.\left.\left. + h\left(x_1^n - x_2^{n-1}\delta t, x_2^{n-1}\right)x_3^{n-1}\right)\delta t\right) - \delta t D_L |k_2|^\alpha\right] \\ &\quad \times \exp\left[-\frac{\tau^2\left(-x_3^n + x_3^{n-1} - \frac{1}{\tau}x_3^{n-1}\delta t\right)^2}{4\delta t D}\right] \\ &\quad \times p\left(x_1^n - x_2^{n-1}\delta t, x_2^{n-1}, x_3^{n-1}, t_{n-1}\right)\mathrm{d}k_2\mathrm{d}x_2^{n-1}\mathrm{d}x_3^{n-1}. \end{aligned} \tag{50}$$

Then the path integral solution is calculated by space partition $[-1 : 0.02 : 1] \times [-1 : 0.02 : 1] \times [-1 : 0.02 : 1]$ and the time-step is 0.01 for the path integral and Monte Carlo solution. The transition probability density function of the path integral method is calculated parallelly by dividing the region into 8 different parts, and the calculation time of each part is about 4428.42 s. The computational cost of Monte Carlo solutions with 2×10^5 sample paths is 3.5998×10^3 s. The marginal probability density function of $p(x_1, x_2)$, $p(x_1, x_3)$, $p(x_2, x_3)$ in Fig. 10 and $p(x_1)$, $p(x_2)$, $p(x_3)$ in Fig. 11 show the good agreement of path integral solutions and Monte Carlo solutions.

In this paper, we mainly derive and verify the path integral solution for n-dimensional SDE under the excitation of α-stable Lévy noise. Specifically, we deduce the short-time transition probability density function required by the path integral method of n-dimensional SDE and prove its correctness. After that, two special examples were selected for numerical implementation, which show the correctness and effectiveness of the derivation. The path integral formulas we derived are obviously valid and usable for higher-dimensional examples when solving the problems of computation and storage, although only three-dimensional examples have been numerically implemented. In order to be able to solve this problem, we can try to convert the problem into an equivalent operation that does not require multiple integrations and storage of large matrices, or solve it with the help of neural networks that have become very popular in recent years for high-dimensional problems.

Declaration of Competing Interest

The authors declare that they have no known competing financial interests or personal relationships that could have appeared to influence the work reported in this paper.

Acknowledgements

This work was supported by the Key International (Regional) Joint Research Program of the National Natural Science Foundation of China (No. 12120101002).

References

[1] Y. Xu, Y.G. Li, H. Zhang, et al., The switch in a genetic toggle system with Lévy noise, Sci. Rep. 6 (2016) 1–11.
[2] Q. Liu, Y. Xu, J. Kurths, Bistability and stochastic jumps in an airfoil system with viscoelastic material property and random fluctuations, Commun. Nonlinear Sci. Numer. Simul. 84 (2020) 105184.
[3] J.Q. Sun, Stochastic dynamics and control, Elsevier, 2006.
[4] F.B. Hanson, Applied Stochastic Processes and Control for Jump-diffusions: Modeling, Analysis and Computation, SIAM, 2007.
[5] S.I. Resnick, Heavy-Tail phenomena: Probabilistic and statistical modeling, Springer Science & Business Media, 2007.
[6] J.Z. Ma, Y. Xu, Y.G. Li, et al., Quantifying the parameter dependent basin of the unsafe regime of asymmetric Lévy-noise-induced critical transitions, Appl. Math. Mech. 42 (2021) 65–84.
[7] W.R. Zan, Y. Xu, J. Kurths, et al., Stochastic dynamics driven by combined Lévy–Gaussian noise: fractional Fokker-Planck-Kolmogorov equation and solution, J. Phys. A 53 (2020) 385001.
[8] J.B. Chen, P.H. Lin, Dimension-reduction of FPK equation via equivalent drift coefficient, Theor. Appl. Mech. Lett. 4 (2014) 013002.
[9] Y. Xu, H. Zhang, Y.G. Li, et al., Solving Fokker-Planck equation using deep learning, Chaos: Interdiscip. J. Nonlinear Sci. 30 (2020) 013133.
[10] M.F. Wehner, W.G. Wolfer, Numerical evaluation of path integral solutions to Fokker-Planck equations, Phys. Rev. A 27 (1983) 2663–2670.
[11] M.F. Wehner, W.G. Wolfer, Numerical evaluation of path integral solutions to Fokker-Planck equations. II. restricted stochastic processes, Phys. Rev. A 28 (1983) 3003–3011.
[12] A. Naess, J.M. Johnsen, Response statistics of nonlinear, compliant offshore structures by the path integral solution method, Probab. Eng. Mech. 8 (1993) 91–106.
[13] J.S. Yu, G.Q. Cai, Y.K. Lin, A new path integration procedure based on Gauss-Legendre scheme, Int. J. Non Linear Mech. 32 (1997) 759–768.
[14] M.D. Paola, G. Alotta, Path integral methods for the probabilistic analysis of nonlinear systems under a white-noise process, ASCE-ASME J. Risk Uncertain. Eng. Syst., Part B: Mech. Eng. 6 (2020) 040801.
[15] A. Naess, V. Moe, Efficient path integration methods for nonlinear dynamic systems, Probab. Eng. Mech. 15 (2000) 221–231.
[16] D.V. Iourtchenko, E. Mo, A. Naess, Response probability density functions of strongly non-linear systems by the path integration method, Int. J. Non Linear Mech. 41 (2006) 693–705.
[17] A. Nasses, C. Skaug, Path integration methods for calculating response statistics of nonlinear oscilators driven by α-stable lévy noise, IUTAM Sympos. Nonlinear Stochastic Struct. Dyn. (1999) 159–169.
[18] M.D. Paola, R. Santoro, Path integral solution for non-linear system enforced by Poisson white noise, Probab. Eng. Mech. 23 (2008) 164–169.
[19] C. Bucher, A.D. Matteo, M.D. Paola, et al., First-passage problem for nonlinear systems under Lévy white noise through path integral method, Nonlinear Dyn 85 (2016) 1445–1456.
[20] A.D. Matteo, A. Pirrotta, Path integral method for nonlinear systems under Lévy white noise, ASCE-ASME J. Risk Uncertain. Eng. Syst., Part B: Mech. Eng. 3 (2017) 030905.
[21] W.R. Zan, Y. Xu, R. Metzler, et al., First-passage problem for stochastic differential equations with combined parametric Gaussian and Lévy white noises via path integral method, J. Comput. Phys. 435 (2021) 110264.
[22] W.R. Zan, W.T. Jia, Y. Xu, Response statistics of single-degree-of-freedom systems with Lévy noise by improved path integral method, Int. J. Appl. Mech. 14 (2022) 2250029.